

PDF hosted at the Radboud Repository of the Radboud University Nijmegen

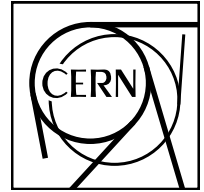
The following full text is a preprint version which may differ from the publisher's version.

For additional information about this publication click this link.

<http://hdl.handle.net/2066/117222>

Please be advised that this information was generated on 2020-09-24 and may be subject to change.

EUROPEAN ORGANISATION FOR NUCLEAR RESEARCH (CERN)



CERN-PH-EP-2012-317

Submitted to: JHEP

Search for third generation scalar leptoquarks in pp collisions at $\sqrt{s} = 7$ TeV with the ATLAS detector

The ATLAS Collaboration

Abstract

A search for pair-produced third generation scalar leptoquarks is presented, using proton–proton collisions at $\sqrt{s} = 7$ TeV at the LHC. The data were recorded with the ATLAS detector and correspond to an integrated luminosity of 4.7 fb^{-1} . Each leptoquark is assumed to decay to a tau lepton and a b -quark with a branching fraction equal to 100%. No statistically significant excess above the Standard Model expectation is observed. Third generation leptoquarks are therefore excluded at 95% confidence level for masses less than 534 GeV.

Search for third generation scalar leptoquarks in pp collisions at $\sqrt{s} = 7$ TeV with the ATLAS detector

The ATLAS Collaboration

ABSTRACT: A search for pair-produced third generation scalar leptoquarks is presented, using proton–proton collisions at $\sqrt{s} = 7$ TeV at the LHC. The data were recorded with the ATLAS detector and correspond to an integrated luminosity of 4.7 fb^{-1} . Each leptoquark is assumed to decay to a tau lepton and a b -quark with a branching fraction equal to 100%. No statistically significant excess above the Standard Model expectation is observed. Third generation leptoquarks are therefore excluded at 95% confidence level for masses less than 534 GeV.

Contents

1	Introduction	1
2	The ATLAS detector	2
3	Monte Carlo simulations	3
4	Physics object identification	4
5	Event selection	5
6	Background estimation	6
6.1	Electron channel	7
6.2	Muon channel	9
6.3	Background summary	10
7	Systematic uncertainties	11
7.1	Object-level uncertainties	11
7.2	Theoretical uncertainties	12
7.3	Background uncertainties	13
7.4	Summary of systematic uncertainties	14
8	Results	14
9	Conclusions	18
10	Acknowledgements	18

1 Introduction

Leptoquarks (LQ) are colour-triplet bosons that carry both lepton and baryon numbers and have a fractional electric charge. They are predicted by many extensions of the Standard Model (SM) [1–7] and may provide unification between the quark and lepton sectors. In accordance with experimental results on lepton-number violation, flavour-changing neutral currents and proton decay, it is assumed that individual leptoquarks do not couple to particles from different generations [8, 9], thus leading to three generations of leptoquarks. The most recent limit on pair-produced third generation scalar leptoquarks (LQ_3) decaying to $\tau b \tau b$ comes from the CMS experiment, in which scalar leptoquarks with masses below 525 GeV are excluded at the 95% confidence level (CL)[10]. Limits have also been set by the D0 [11] and CDF [12] experiments at the Tevatron, which have excluded third generation scalar leptoquarks with masses up to 210 GeV and 153 GeV respectively. First and second generation scalar leptoquarks have been excluded up to 830 GeV and 840

GeV respectively [13–15]. The results presented here are based on a total integrated luminosity of 4.7 fb^{-1} of proton-proton collision data at a centre-of-mass energy of $\sqrt{s} = 7 \text{ TeV}$, collected by the ATLAS detector at the LHC during 2011. The final states investigated arise from the decay of both leptoquarks into a tau lepton and a b -quark, leading to a $\tau b \tau b$ final state. The branching fraction of LQ_3 decays to τb is assumed to be equal to 100%.

Tau leptons can decay either leptonically (to an electron or muon plus two neutrinos), or hadronically (typically to one or three charged hadrons, plus one neutrino, and zero to four neutral hadrons). Since the final state includes two taus, this leads to three possible sub-categories of events: di-lepton, lepton–hadron and hadron–hadron. Of these, the lepton–hadron category has the largest branching fraction (45.6%), and the presence of one charged light lepton ($\ell = e, \mu$) in the event is useful for event triggering and provides better rejection of the multi-jets background. Only the lepton–hadron decay mode is considered in this analysis, resulting in either an $e \tau_{\text{had-vis}} bb + 3\nu$ or $\mu \tau_{\text{had-vis}} bb + 3\nu$ final state, where $\tau_{\text{had-vis}}$ refers to the visible (non-neutrino) components of the hadronic tau decay.

Selected events are therefore required to have one electron or muon with large transverse momentum (p_T), one high- p_T hadronically decaying tau, missing transverse energy from the tau decays, and two high- p_T jets. Searches are performed independently for the electron and muon channels. The results are subsequently combined and interpreted as lower bounds on the LQ_3 mass.

2 The ATLAS detector

The ATLAS detector [16] is a multi-purpose detector with a forward-backward symmetric cylindrical geometry and nearly 4π coverage in solid angle. ATLAS uses a right-handed coordinate system with its origin at the nominal interaction point (IP) and the z -axis along the beam pipe. The x -axis points from the IP to the centre of the LHC ring, and the y -axis points upward. Cylindrical coordinates (r, ϕ) are used in the transverse (x, y) plane, with ϕ being the azimuthal angle around the beam pipe. The pseudorapidity η is defined in terms of the polar angle θ by $\eta = -\ln(\tan(\theta/2))$. The three major sub-components of ATLAS are the tracking detector, the calorimeter and the muon spectrometer.

Charged particle tracks and vertices are reconstructed using silicon pixel and microstrip detectors covering the range $|\eta| < 2.5$, and by a straw tube tracker that covers $|\eta| < 2.0$. Electron identification capability is added by employing Xenon gas to detect transition radiation photons created in a radiator between the straws. The inner tracking system is immersed in a homogeneous 2 T magnetic field provided by a solenoid.

Electron, jet and tau energies are measured in the calorimeter. The ATLAS calorimeter system covers a pseudorapidity range of $|\eta| < 4.9$. Within the region $|\eta| < 3.2$, electromagnetic calorimetry is provided by barrel and end-cap high-granularity lead/liquid argon (LAr) electromagnetic (EM) calorimeters, with an additional thin LAr presampler covering $|\eta| < 1.8$, to correct for energy loss in material upstream of the calorimeters. Hadronic calorimetry is provided by a steel/scintillator-tile calorimeter, segmented into three barrel structures within $|\eta| < 1.7$, and two copper/LAr hadronic end-cap calorimeters. The forward region ($3.1 < |\eta| < 4.9$) is instrumented by a LAr calorimeter with copper (EM) and tungsten (hadronic) absorbers.

Surrounding the calorimeters, a muon spectrometer with air-core toroids, a system of precision tracking chambers providing coverage over $|\eta| < 2.7$, and detectors with triggering capabilities over $|\eta| < 2.4$ to provide precise muon identification and momentum measurements.

A three-level event-triggering system selects inclusive electron and muon candidates to be recorded for offline analysis.

3 Monte Carlo simulations

Simulated signal events are produced using the PYTHIA 6.425 [17] event generator with underlying-event Tune D6 [18] and CTEQ6L1 [19] parton distribution functions (PDFs). The coupling $\lambda_{LQ \rightarrow lq}$ which determines the LQ lifetime and width [20] is set to $0.01 \times 4\pi\alpha$, where α is the fine-structure constant. This value is widely used in leptoquark searches and gives the leptoquark a full width of less than 1 MeV and a decay length of less than 1 mm. The signal process is normalised using next-to-leading-order (NLO) cross-sections for scalar leptoquark pair production [21]. The signal production cross-section for a leptoquark mass of 500 GeV is 46.2 fb.

Background processes considered in this analysis are the production of W +jets, Z/γ^* +jets, $t\bar{t}$, single top quarks, boson pairs, and multi-jets. The W - and Z -boson processes are simulated using the ALPGEN 2.13 generator [22] with the technique described in ref. [23] to match the hard process (calculated with a leading-order (LO) matrix element for up to five partons) to the parton shower of HERWIG 6.510 [24], and uses JIMMY 4.31 [25] to model the underlying event. Wherever available, dedicated ALPGEN 2.13 samples with massive charm and bottom partons were used for the W +jets and Z/γ^* +jets processes. All samples listed above are generated using the CTEQ6L1 PDFs. Di-boson processes (WW , WZ , and ZZ) are modelled with HERWIG 6.510 using the MRST [26] LO PDFs. Samples of top-quark pair production and associated production of single top quark (Wt) events are produced using the MC@NLO 4.01 [27–30] generator interfaced with HERWIG 6.510 for parton showering, and JIMMY 4.31 to model the underlying event. The CT10 [31] PDFs are used. Single-top s - and t -channel processes are modelled with AcerMC 3.8 [32] using the MRST LO PDFs. The top-quark mass is taken as 172.5 GeV. In all simulated samples TAUOLA [33] and PHOTOS [34] are used to model τ -lepton decays and additional photon radiation from charged leptons, respectively. The W +jets and Z +jets samples are normalised to the inclusive NNLO cross-sections in the proportions predicted by NLO calculations for exclusive n -parton production. The most precise available calculation (nearly NNLO) is used to normalise $t\bar{t}$ production [35]. All other sources of background are normalised using the cross-sections calculated at NLO.

Signal and background events are processed through a detailed detector simulation [36] based on GEANT4 [37]. The data used in this paper are affected by multiple pp collisions occurring in the same or neighbouring bunch crossings (pile-up) and have an average of ten interactions per bunch crossing. The effects of pile-up are taken into account by overlaying simulated minimum-bias events onto the simulated hard-scattering events. The Monte Carlo (MC) samples are then re-weighted such that the average number of pile-up interactions matches that seen in the data.

4 Physics object identification

Collision events are required to have at least one reconstructed vertex with at least four associated tracks with $p_T > 0.4$ GeV. In events where more than one vertex is found, the primary vertex is defined as the one with the highest $\sum p_T^2$ of the associated tracks. For the final state of interest described below, this choice of primary vertex is correct in 98.9% (98.4%) of the cases in the electron (muon) channel for the luminosity range considered here.

Electron candidates are reconstructed from clusters of cells in the electromagnetic calorimeter and from tracks in the inner detector. They are required to pass a set of electron identification cuts, based on information about the transverse shower shape, the longitudinal leakage into the hadronic calorimeter, transition radiation, and the requirement that a good-quality track with a hit in the innermost pixel layer points to the calorimeter cluster [38]. A tight working point corresponding to a selection efficiency of approximately 80% for true electrons in simulation is chosen. Electrons are required to have $p_T > 20$ GeV and $|\eta| < 2.47$, excluding the transition region between the barrel and the end-cap calorimeters, *i.e.* $1.37 < |\eta| < 1.52$. Isolation requirements are placed on the electron candidates by demanding that the calorimeter transverse energy in a cone of radius $\Delta R = 0.2$ around the electron (not including the electron cluster) must be less than 20% of the electron p_T , where $\Delta R = \sqrt{(\Delta\eta)^2 + (\Delta\phi)^2}$. In addition, track isolation is imposed by requiring that the p_T sum of additional tracks (not including the electron track) in a cone of radius $\Delta R = 0.2$ is less than 20% of the electron track p_T .

Muon tracks are reconstructed independently in the inner detector and in the muon spectrometer. Tracks are required to have a minimum number of hits in each, and must be compatible in terms of geometrical and momentum matching. The information from both systems is then used in a combined fit to refine the measurement of the momentum of each muon. Muon candidates are required to have $p_T > 20$ GeV and $|\eta| < 2.5$. The average muon reconstruction efficiency is approximately 90%, except for small regions in pseudorapidity where it drops to 80% [39]. Isolation requirements are imposed by demanding that the transverse energy (E_T) deposited in the calorimeter in a cone of radius $\Delta R = 0.2$ around the muon (not including the cells crossed by the muon) is less than 20% of the muon p_T . Furthermore, track isolation is imposed by requiring that the p_T sum of additional tracks (not including the muon track) in a cone of radius $\Delta R = 0.2$ be less than 20% of the muon p_T .

Jets are reconstructed using the anti- k_t [40] algorithm with a radius parameter $R = 0.4$. The jet algorithm is run on calibrated topological clusters of calorimeter cells [41]. Additional p_T - and η -dependent corrections are applied to jets to bring them to the final calibrated energy scale [42]. Selected jets must have $p_T > 25$ GeV and $|\eta| < 2.8$.

The identification of jets originating from b -quarks is performed using a neural-network-based tagger [43] that uses the output weights of several likelihood-based algorithms as inputs. The track transverse and longitudinal impact parameters with respect to the primary vertex are examples of variables used by these algorithms. A working point corresponding to an identification efficiency of approximately 70% for true b -jets in simulation is chosen. For jets initiated by gluons or light quarks, the rejection factor (1/fraction that pass the b -tagging ID) is of order 100.

The reconstruction of hadronically decaying tau leptons is seeded by jets which are reconstructed within the acceptance of the inner detector. Only clusters in a cone with radius $\Delta R = 0.2$

are used to define the visible tau energy and direction because the products of hadronic tau decays are more collimated than those from multi-jet processes. Additional corrections depending on the p_T , η and number of tracks are applied to bring the reconstructed tau candidates to the correct energy scale [44]. The energy deposition in the calorimeter is required to be matched to either one or three tracks in the inner detector. Hadronically decaying taus are required to have visible $p_T > 20$ GeV, $|\eta| < 2.5$ and unit charge, and are identified using a Boosted Decision Tree (BDT)¹ [45] which uses both calorimeter and tracking-based variables such as shower width and track multiplicity. A working point with an identification efficiency for true hadronic tau decays in simulation of $\sim 50\%$ is chosen. The rejection factor for jets ranges from 50 to 100 depending on the number of tracks matching the jet candidate.

The missing transverse momentum is a two-dimensional vector defined as the negative vector sum of the transverse momenta of reconstructed electrons, muons, tau leptons and jets, and also of calorimeter energy deposits not associated with reconstructed objects.² The magnitude of the missing transverse momentum vector is referred to as the missing transverse energy (E_T^{miss}).

5 Event selection

Events are required to be identified by the trigger system as containing at least one electron or one muon. In order to control the data-taking bandwidth, the trigger system imposed a minimum transverse energy threshold on electrons of 20 GeV or 22 GeV (depending on the data-taking period), and a minimum p_T threshold on muons of 18 GeV. For the highest luminosities towards the end of the data-taking period, the muon trigger is required to be accompanied by a jet that passes the first-level trigger p_T threshold of 10 GeV. All data events are required to be recorded during stable LHC running conditions and with all relevant sub-detectors functioning normally. Events are cleaned for instrumental effects, such as sporadic noise bursts [46].

Events are required to have exactly one reconstructed electron (muon) with $p_T > 25$ (20) GeV. This suppresses background processes such as $Z/\gamma^* \rightarrow \ell\ell$ and $t\bar{t}$ which have a higher average lepton multiplicity. Exactly one identified hadronic tau decay candidate with $p_T > 30$ GeV and opposite-sign charge to the lepton is required. The E_T^{miss} is required to be larger than 20 GeV in order to further reject multi-jet and $Z/\gamma^* \rightarrow \ell\ell$ processes. In addition, at least two reconstructed jets are required, with the leading jet having $p_T > 50$ GeV and the sub-leading jet having $p_T > 25$ GeV.

The signal-to-background ratio is improved by requiring that either the leading or sub-leading jet passes the b -tagging requirements. After requiring that events must have one of these two jets passing the b -tagging requirements, the dominant background process is $t\bar{t}$. Since both the signal and $t\bar{t}$ processes contain two b -jets in the final state, no further improvement in sensitivity is obtained by requiring that a second jet in the event also pass the b -tagging requirements.

The visible mass ($m_{\tau_{\text{had-vis}}-\text{jet}}$) of the tau candidate and the closest jet in $\eta - \phi$ space (minimum ΔR) is required to be larger than 90 GeV. Only jets with $p_T > 40$ GeV are considered. This cut

¹A BDT is a multivariate analysis technique where the selection is based on a majority vote on the result of several decision trees, each of which is derived from the same training sample by supplying different event weights during the training.

²Energy deposits in the calorimeters are expressed as four-vectors (E, \mathbf{p}) , where the direction is determined from the position of the calorimeter cluster and the position of the primary vertex.

is chosen to reject semi-leptonic $t\bar{t}$ events where the tau candidate is faked by jets from $W \rightarrow q\bar{q}$ decays.

In events containing leptoquark decays, large E_T^{miss} arises from neutrinos accompanying the tau decays. Taus originating from leptoquarks typically have high momentum, thus the decay products are predominantly collinear and the E_T^{miss} direction is correlated with the direction of the visible tau decay products. Two variables are defined in order to improve the separation of signal and background: the absolute difference in ϕ between the charged lepton and E_T^{miss} ($|\Delta\phi(E_T^{\text{miss}}, \ell)|$), and the absolute difference in ϕ between the tau candidate and E_T^{miss} ($|\Delta\phi(E_T^{\text{miss}}, \tau_{\text{had-vis}})|$). The relationship between these two variables for simulated signal ($m_{LQ} = 500 \text{ GeV}$) and the dominant top background, after applying all the requirements described above is shown in figure 1. Events must satisfy the following requirement:

$$|\Delta\phi(E_T^{\text{miss}}, \ell)| \leq -\frac{1.5}{\pi} |\Delta\phi(E_T^{\text{miss}}, \tau_{\text{had-vis}})| + 2 \text{ (radians)}, \quad (5.1)$$

where $\ell = e, \mu$. This E_T^{miss} angular requirement selects events below the solid line in figure 1. A leptonically decaying tau is accompanied by two neutrinos, whereas a hadronically decaying tau is accompanied by only one. In events with two true taus (as in the signal process), the E_T^{miss} is therefore typically aligned with the leptonic tau decay and these events are preferentially selected by the E_T^{miss} angular requirement. The signal efficiency is approximately 85%, independent of leptoquark mass. For $t\bar{t}$ events containing a real hadronic tau (produced from the W decay), the additional neutrinos from the tau decay cause the E_T^{miss} to be preferentially aligned with the hadronic tau decay and these are rejected. In the subset of $t\bar{t}$ events where the tau is faked by a jet from W -decay, events are evenly distributed across the $|\Delta\phi(E_T^{\text{miss}}, \ell)| - |\Delta\phi(E_T^{\text{miss}}, \tau_{\text{had-vis}})|$ plane and a large proportion of these are also rejected. The overall efficiency for inclusive $t\bar{t}$ events is 31%.

6 Background estimation

Backgrounds considered in this analysis are the production of W +jets and Z/γ^* +jets (collectively referred to as V +jets), $t\bar{t}$, single top quarks, di-boson and multi-jets. Normalisation factors are applied to the MC predictions for V +jets and top backgrounds in background-enriched control regions, to predict as accurately as possible the background in the signal region, as described in more detail below. These control regions are constructed to be mutually exclusive of the signal region and the assumption is made that normalisation factors in the signal region are the same as in the background-enriched control regions. The contribution from multi-jets is estimated using fully data-driven techniques. The contribution from di-boson processes is taken directly from MC. The shapes of the distributions are taken from simulation in the signal region.

Different approaches are used to estimate the backgrounds in the electron and muon channels. Normalisation factors for the electron channel are calculated after applying the electron, tau, E_T^{miss} , charge-product cuts, and jet multiplicity and p_T requirements described in section 5 above. This approach minimises bias with respect to the signal region, but leads to limited statistics (for MC and data) in the control regions. Normalisation factors for the muon channel are calculated after applying only the muon, tau and charge-product requirements described in section 5.

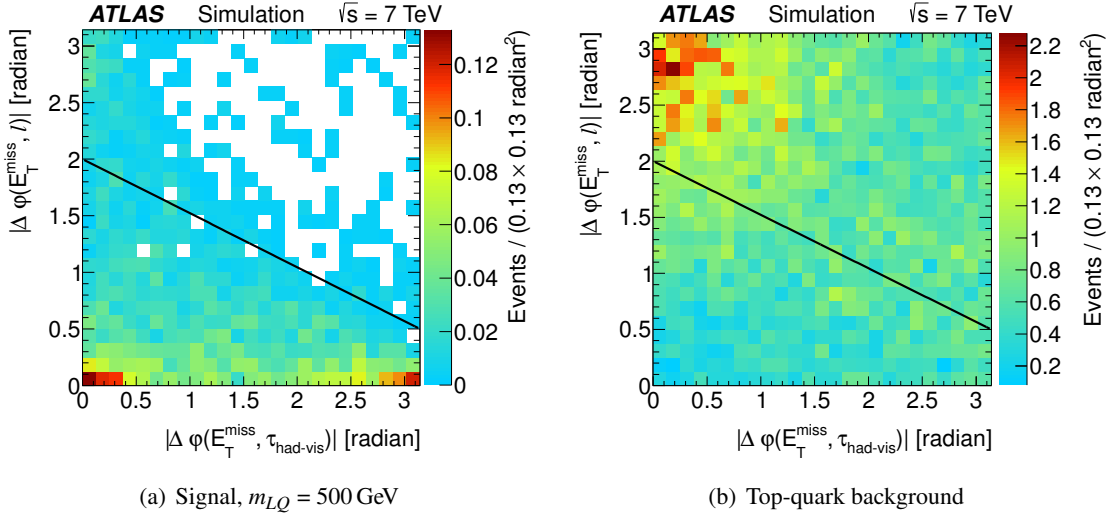


Figure 1. The absolute value of the angle $\Delta\phi$ between the reconstructed charged light lepton and E_T^{miss} as a function of $|\Delta\phi|$ between $\tau_{\text{had-vis}}$ and E_T^{miss} for simulated (a) signal ($m_{LQ} = 500$ GeV) and (b) top-quark background, after applying all selection cuts (see text) and normalising to the integrated luminosity of the data. The function corresponding to the solid line is defined in eq. 5.1.

6.1 Electron channel

The multi-jets background is estimated by defining a region in data with a tau candidate that fails the tau BDT identification used in the nominal selection but passes a looser identification working point, and has the same-sign charge as the electron. In addition, the events are required not to contain any taus that pass the nominal selection criteria. Contributions from W , Z/γ^* +jets, top-quark, and di-boson background processes estimated from MC simulations are subtracted to get the shape of the multi-jets distribution. The normalisation is determined by performing a two-component maximum likelihood fit to kinematic distributions of the sum of multi-jets and all other sources of background to data, with the multi-jets fraction being the fit parameter. The variable used for fitting is chosen to provide good discrimination between multi-jets and other sources of background. The method is used to calculate the multi-jets contribution in the signal region, where the transverse mass between the charged light lepton and the E_T^{miss} , defined to be:

$$m_T = \sqrt{2p_T^\ell E_T^{\text{miss}}(1 - \cos(\Delta\phi))}, \quad (6.1)$$

is used as the fit variable. The multi-jets contribution is found to be $12_{-16}^{+8}\%$ of the total data yield in the signal region. The same method is also used in background control regions, fitting to the E_T^{miss} distribution in the W and $Z/\gamma^* \rightarrow \tau\tau$ control regions, and the electron E_T in the top control region. The validity of the method used to estimate the multi-jets background contribution is cross-checked by using events with same-sign charge electron–tau pairs as the control region and found to be compatible within statistical errors. Dependence on the choice of variable used is evaluated by fitting to other kinematic variables, and also found to be within statistical errors of the nominal value.

$Z/\gamma^* \rightarrow ee+\text{jets}$	Require one extra electron
$Z/\gamma^* \rightarrow \tau\tau+\text{jets}$	b -jet veto $40 < m_{e\tau_{\text{had-vis}}} < 80 \text{ GeV}$ $m_T < 60 \text{ GeV}$
$W+\text{jets}$	b -jet veto Fail E_T^{miss} angular cut $60 < m_T < 120 \text{ GeV}$
Top-quark	b -jet requirement $m_{\tau_{\text{had-vis},jet}} > 90 \text{ GeV}$ Fail E_T^{miss} angular cut $S_T < 350 \text{ GeV}$

Table 1. Control region definitions for the electron channel. The electron, tau, charge-product, E_T^{miss} , and jet multiplicity and p_T requirements are applied as described in section 5.

Separate control regions are defined for the $Z/\gamma^* \rightarrow ee$, $Z/\gamma^* \rightarrow \tau\tau$, W , and $t\bar{t}$ and single top-quark processes. They are defined by applying the electron, tau, charge-product, E_T^{miss} , and jet multiplicity and p_T requirements (as described in section 5, collectively referred to as the ‘baseline’ requirements), in addition to the cuts shown in table 1.

The control region for $Z/\gamma^* \rightarrow ee$ events is constructed by requiring an additional electron with $p_T > 20 \text{ GeV}$ and opposite-sign charge to the first one. The second electron is required to pass the same identification requirements as the first one.

The $Z/\gamma^* \rightarrow \tau\tau$ control region is defined by additionally requiring that the visible mass of the electron–tau pair is in the range $40 < m_{e\tau_{\text{had-vis}}} < 80 \text{ GeV}$ and that the transverse mass between the electron and the E_T^{miss} is less than 60 GeV . A b -jet veto is also applied, using a looser working point (with a selection efficiency of 75%) compared to the working point used for signal selection. In this way contamination from top backgrounds is reduced.

The $W+\text{jets}$ control region is constructed by applying in addition a b -jet veto (as described above), demanding that $60 < m_T < 120 \text{ GeV}$, and requiring that the event fail the E_T^{miss} angular requirements cut (eq. 5.1).

The control region for top backgrounds is defined by additionally requiring that events pass the b -tagging requirements, have $m_{\tau_{\text{had-vis},jet}} > 90 \text{ GeV}$, fail the E_T^{miss} angular requirements and have $S_T < 350 \text{ GeV}$, where S_T is defined as the scalar sum of the p_T of the charged light lepton, the tau, the two highest- p_T jets and the E_T^{miss} in the event,

$$S_T = p_T^{e/\mu} + p_T^{\tau_{\text{had-vis}}} + p_T^{\text{jet1}} + p_T^{\text{jet2}} + E_T^{\text{miss}}. \quad (6.2)$$

Normalisation factors for $V+\text{jets}$ and top backgrounds in the electron channel are calculated according to:

$$NF_{\text{BG}} = \frac{N^{\text{Data}} - N_{\text{OtherBG}}^{\text{MC}}}{N_{\text{BG}}^{\text{MC}}}, \quad (6.3)$$

where N^{Data} is the number of data events in the control region, $N_{\text{OtherBG}}^{\text{MC}}$ is the expected number of events from other background processes, and $N_{\text{BG}}^{\text{MC}}$ is the contribution in the control region from

the background process of interest.

To account for contamination from other background processes in the control regions, normalisation factors are found for each region in turn. At each stage the multi-jets contribution is re-estimated and all previously found normalisation factors are applied when estimating the contribution from other background processes.

The final background normalisation factors obtained are presented in table 3 and discussed together with the muon channel in section 6.3.

6.2 Muon channel

The multi-jets contribution to the control and signal regions are estimated in the muon channel from data using the ABCD method. Events are sorted into four regions using two observables assumed to be independent – the muon isolation and the sign of the charge product of the muon–tau pair. The regions are therefore defined as: isolated muon and opposite-sign muon–tau pair (A), isolated muon and same-sign muon–tau pair (B), as well as two regions with a non-isolated muon and opposite-sign or same-sign charge muon–tau pair (C and D respectively). Non-isolated muons are defined as those which fail at least one of the isolation requirements described in section 5. Contributions from other physics processes in regions B , C , and D are subtracted using the MC simulation. The shape of kinematic distributions for the multi-jets background is taken from region B , while the expected number of events in the signal region (A) is determined by taking the product of the number of events in region B with the ratio of the number of events in regions C and D (*i.e.* $N_A = N_B \times \frac{N_C}{N_D}$). The multi-jets contribution is estimated to be $15 \pm 4\%$ of the total data yield in the signal region. The validity of the method is checked by varying both isolation cuts up and down from the nominal value of 0.2 by 0.05. Deviations in the ratio $\frac{N_C}{N_A}$ are included as an additional systematic uncertainty.

Control regions for V +jets and top-quark background processes are defined by applying the muon and tau requirements (including the charge-product requirement) as described in section 5. Additional selection criteria used for each control region are listed in table 2. Normalisation factors are calculated for each process by performing a maximum likelihood fit. The variable used for fitting is chosen in each case to provide good discrimination between the background process of interest, and other contributing physics processes in that control region. The contribution from multi-jets in each control region is estimated using the method described above, and this and contributions from other background processes are taken into account when performing the fits.

The control region for $Z/\gamma^* \rightarrow \mu\mu$ events is defined by requiring two oppositely charged muons and one hadronic tau decay. The second muon is required to pass the same requirements as the first. The normalisation factor for $Z/\gamma^* \rightarrow \mu\mu$ events in the signal region is then determined by fitting to the di-muon invariant mass distribution in the range $60 < m_{\mu\mu} < 120$ GeV.

The normalisation of $Z/\gamma^* \rightarrow \tau\tau$ events is obtained by selecting events with one muon, one hadronic tau decay and $E_T^{\text{miss}} > 20$ GeV. Additionally, events are required to fail the b -jet requirement. The fit is performed using the visible mass of the muon–tau pair in the range $45 < m_{\mu\tau_{\text{had-vis}}} < 80$ GeV.

The control region for W +jets events is defined by selecting events with one muon, one hadronic tau decay and $E_T^{\text{miss}} > 20$ GeV, and which fail the b -jet requirement. The normalisa-

$Z/\gamma^* \rightarrow \mu\mu+\text{jets}$	Require one extra muon $60 < m_{\mu\mu} < 120 \text{ GeV}$
$Z/\gamma^* \rightarrow \tau\tau+\text{jets}$	$E_T^{\text{miss}} > 20 \text{ GeV}$ b -jet veto $45 < m_{\mu\tau_{\text{had-vis}}} < 80 \text{ GeV}$
$W+\text{jets}$	$E_T^{\text{miss}} > 20 \text{ GeV}$ b -jet veto $70 < m_T < 100 \text{ GeV}$
Top-quark	$E_T^{\text{miss}} > 20 \text{ GeV}$ $p_T^{\text{jet1}} > 50 \text{ GeV}$ b -jet requirement $m_{\tau_{\text{had-vis}}-\text{jet}} > 90 \text{ GeV}$ Fail E_T^{miss} angular cut $S_T < 350 \text{ GeV}$

Table 2. Control region definitions for the muon channel. The muon, tau and charge-product requirements are also applied as described in section 5.

Background	Electron channel	Muon channel
$Z/\gamma^* \rightarrow \ell\ell+\text{jets}$	0.54 ± 0.09	0.52 ± 0.02
$Z/\gamma^* \rightarrow \tau\tau+\text{jets}$	0.99 ± 0.08	1.00 ± 0.02
$W+\text{jets}$	0.63 ± 0.07	0.50 ± 0.01
$t\bar{t}$ and single-top	0.92 ± 0.08	0.93 ± 0.09

Table 3. Summary of background normalisation factors obtained using the control regions specified in tables 1 and 2. The errors include both the statistical and systematic (discussed in section 7.3) uncertainties.

tion is determined by fitting to the transverse mass of the charged light lepton and the E_T^{miss} in the range $70 < m_T < 100 \text{ GeV}$.

The control region for $t\bar{t}$ and single-top processes is defined by applying all selection criteria, with the exception of the E_T^{miss} angular requirement which is reversed. In addition, the S_T of the event is required to be less than 350 GeV. The normalisation factor is obtained by fitting to the S_T distribution up to 350 GeV.

6.3 Background summary

The background normalisation factors in the signal region determined from data for both channels are presented in table 3.

Uncertainties for normalisation factors are larger in the electron channel than the muon channel due to the tighter requirements placed on the control region definitions, namely the additional requirements on E_T^{miss} and jets which are not applied for the muon channel (unless explicitly stated).

As a cross-check, the electron channel method (detailed in section 6.1) is applied to the muon channel and the signal region normalisation factors determined in this way are found to be

$NF_{Z/\gamma \rightarrow \mu\mu} = 0.59 \pm 0.09$, $NF_{Z/\gamma \rightarrow \tau\tau} = 1.03 \pm 0.08$, $NF_W = 0.50 \pm 0.08$ and $NF_{\text{top}} = 0.93 \pm 0.09$. These figures agree within uncertainties with the factors determined using the method described in section 6.2 and shown in table 3.

The largest background contribution comes from $t\bar{t}$ events, with approximately 55% of these coming from events containing a real hadronic tau decay (from the W decay) after all selection cuts are applied. Approximately 40% come from events where the W boson decays hadronically, and the tau candidate is faked by one of the jets. In the remaining $\sim 5\%$ of events, the reconstructed hadronic tau decay is faked in equal proportions by electrons or b -jets. Normalisation factors for background processes in which the hadronic tau decay is faked by a jet are observed to be significantly smaller than unity. This is a known effect, caused by jets being narrower in simulation than in data and therefore being more likely to fake a hadronic tau decay [47].

In both methods used for background estimation, the control regions for V +jets background processes either make no requirements on b -tagging, or veto events containing one or more b -jets. Simulation tests have validated the assumption that the normalisation factors obtained in regions that require b -jets are the same as those in regions where b -jets are not explicitly required, or are vetoed.

7 Systematic uncertainties

In simulated samples all sources of uncertainty are varied individually within their errors and the impact on the results of the analysis is determined. Background normalisation factors and multi-jets contributions are recalculated for each source of systematic uncertainty. In this way the nominal simulation (comprising the current best estimates for physics object reconstruction corrections) and systematic variations are treated coherently, and the uncertainties are propagated through the analysis. The S_T distribution is used to test for the existence of leptoquarks, since this variable provides the best discrimination between signal and background (discussed further in section 8). The shape of the S_T distribution remains unchanged within the total shape uncertainty (see further discussion in section 8) when applying all the uncertainties detailed below and systematic variations are therefore treated as nuisance parameters affecting the overall scale. The relative changes in acceptance for signal and background are quoted for each systematic variation.

7.1 Object-level uncertainties

There are several sources of systematic uncertainty associated with the reconstruction, identification, and energy scale of physics objects, which can potentially affect the estimated shapes of kinematic distributions and the normalisation of various processes.

Uncertainties associated with the efficiency of single-lepton triggers are typically less than 1% [48, 49] and a $\pm 0.5\%$ ($\pm 3.3\%$) variation in the signal acceptance is observed when varying the electron (muon) trigger efficiency by $\pm 1\sigma$. The effect on background processes is negligible.

Varying the electron energy scale by $\pm 1\sigma$ results in a $\pm 0.8\%$ change in background acceptance compared to the nominal selection and has a negligible impact on the signal yields. The electron reconstruction and identification efficiency uncertainties are combined in quadrature and yield an overall change of less than 1.5% for both signal and background.

Varying the muon momentum scale by 1σ results in a 0.2% change in signal yields compared to the nominal selection. The impact of muon resolution uncertainties on signal and background acceptance is found to be negligible. A $\pm 1\sigma$ variation of muon reconstruction efficiency results in a $\pm 0.3\%$ change in signal acceptance.

The uncertainty on the tau energy scale is typically around 3%, depending on the p_T and η of the hadronically decaying tau candidate [50]. Varying the energy scale by $\pm 1\sigma$ changes the acceptance for background and low-mass signal ($m_{LQ} = 200$ GeV) by approximately 2%, decreasing to 1.2% for $m_{LQ} = 500$ GeV. The uncertainty on the tau identification efficiency is 4% for taus with $p_T < 100$ GeV. This increases linearly with p_T up to a maximum of 8% for three-prong taus with $p_T > 350$ GeV. Varying the tau identification efficiency by this uncertainty results in an overall acceptance change for signal of approximately 6% (for a leptoquark of mass 500 GeV). The variation of background yields is found to be approximately 1% – significantly smaller than the change in the signal yield, because the effect is largely absorbed in the normalisation factor defined in the control region.

The jet energy resolution uncertainty is approximately 10% and affects the event yields by approximately 2% [42]. The jet energy scale uncertainty depends on p_T and η , and varies between 2% and 5%. It is modelled by 14 separate nuisance parameters, each of which is varied by $\pm 1\sigma$ independently from the others. The use of control regions does not significantly reduce the variations of the different background yields, and changes in acceptance of signal and background of up to $\pm 2\%$ are observed.

The uncertainty on the b -jet identification efficiency for the algorithm and operating point used in this analysis ranges from 5% to 18% depending on jet kinematics. The b -tagging efficiency and probability that a light jet is identified as a b -jet are anti-correlated and thus varied accordingly. A $\pm 1\sigma$ variation results in a $\pm 9\%$ ($\pm 15\%$) change in signal acceptance for leptoquarks with a mass of 200 (500) GeV. The use of control regions reduces the background yield variation to $\pm 3\%$ in both channels.

All energy scale and resolution corrections for electron, muon, tau and jet candidates are propagated consistently to the E_T^{miss} calculation. Additional uncertainties related to the energy scale and pile-up dependence of calorimeter clusters not associated with any high- p_T objects (electrons, taus, jets) are also considered in the E_T^{miss} calculation. These sources are varied independently within their uncertainties and the impact on signal and background yields is found to be negligible.

The uncertainty on the integrated luminosity for data taken during 2011 is $\pm 3.7\%$ as determined in ref. [51].

7.2 Theoretical uncertainties

QCD renormalisation and factorisation scales are varied by a factor of two to estimate the impact on the signal production cross-section. The variation is found to be $\pm 12\%$. A re-weighting technique is used to assess the sensitivity of the signal acceptance to the choice of parton distribution functions and the resulting uncertainty is estimated to be $\pm 12\%$. Varying the multi-parton interactions within experimental bounds has a negligible effect on the signal process.

The effect of the choice of event generator for the top-quark background is estimated by using PowHeg 1.0 [52, 53] (instead of MC@NLO 4.01) to model the hard process. The parton shower and hadronisation models, and the underlying event model (respectively HERWIG 6.510

and JIMMY 4.31 in the nominal sample) are replaced with those from PYTHIA 6.425. In addition, the CTEQ6L1 PDF set is used instead of CT10 which is used in the nominal $t\bar{t}$ sample. The total background yield is found to differ by 1.5% with respect to the nominal samples.

The uncertainty on the signal and the top-quark background due to initial-state radiation (ISR) and final-state radiation (FSR) is evaluated using the AcerMC generator interfaced to the PYTHIA 6.425 shower model with the parameters controlling ISR and FSR varied in a range consistent with experimental data [54]. The event yields are found to agree with nominal values within statistical uncertainties.

MC@NLO events with top-quark masses of 170 GeV and 175 GeV are used to assess the top-quark mass dependence, which is added in quadrature to the uncertainty related to the choice of event generator and PDF set. The resulting uncertainty (2.8%) is treated as a nuisance parameter affecting the background yield and is assumed to be fully correlated between the electron and muon channels.

Other background processes taken from simulation (W , Z/γ^* , di-boson) account for less than 20% of the total background. The W and Z/γ^* samples are simulated with the matching parameter (described in ref. [23]) set to 20 GeV. Event yields are found to agree with the nominal values within statistical uncertainties when this parameter is changed to 30 GeV.

The W and Z control regions are defined with either the application of a b -jet veto, or with no b -tagging requirements. The uncertainties on the production cross-sections of W or Z bosons in association with one or two b -jets are estimated using MCFM [55, 56]. The QCD renormalisation and factorisation scales are varied independently by a factor of two, and different PDF sets are considered. The total uncertainty is found to be 30% and the uncertainties on the normalisation factors for W and Z background processes are increased by this amount (*i.e.* to 2%).

7.3 Background uncertainties

For each channel, the systematic uncertainties on the normalisation factors in table 3 are evaluated by calculating the normalisation factor for a given background when normalisation factors for all other sources of background are varied up or down by their statistical error. The systematic uncertainty on the multi-jets background is evaluated by varying the normalisation factors of other backgrounds by $\pm 1\sigma$. The methods used to estimate the contributions from multi-jets processes are validated by modifying the control regions used, and in the case of the electron channel the variable used for fitting (see sections 6.1 and 6.2). Deviations from the nominal value are included as additional sources of systematic uncertainty.

Conservatively, all background normalisation factors are assumed to be fully correlated and the impact on the total background yield is $^{+16}_{-19}\%$ for the electron channel and $\pm 9\%$ for the muon channel. The background estimation method used in the muon channel allows a more accurate determination of the normalisation factors compared to the event-counting method employed in the electron channel, and the normalisation factor uncertainty for the muon channel is correspondingly smaller than in the electron channel. For both channels, the limited number of data events in the top-quark control region is the main source of uncertainty on the top-quark normalisation factor, which in turn has the largest impact on the total yield uncertainty. Due to the tighter requirements on control regions for the electron channel background estimation, this method also suffers from a

	Background	LQ($m=500$ GeV)
Luminosity	–	3.7
Theory	2.8	17
Normalisation factors	+16/ – 19	–
Trigger efficiency	< 0.2	0.5
Electron energy scale	0.8	0.4
Electron reconstruction and identification efficiency	1.5	1.5
Tau energy scale	2.6	1.2
Tau ID efficiency	1.2	5.7
Jet energy scale (nuisance parameter dependent)	0.1 – 2.4	< 0.2
Jet energy resolution	2.5	0.3
b -tagging efficiency	2.7	15

Table 4. The sources of systematic uncertainty in the electron channel and the relative change (in %) in the background and signal yields. The theory term includes uncertainties related to initial and final state radiation, PDFs, and multi-parton interactions.

limited number of events in data and simulation when estimating normalisation factors for V +jets background processes.

7.4 Summary of systematic uncertainties

The shape of the S_T distribution remains unchanged within statistical uncertainties when applying all the uncertainties mentioned above. The uncertainties for the electron and muon channels are summarised in tables 4 and 5 respectively. Uncertainties related to the background normalisation factors have the largest impact on the total background yield, while for the signal yield the largest sources of systematic uncertainty are due to theoretical uncertainties (comprising uncertainties related to PDFs, multi-parton interactions, and initial- and final-state radiation) and from b -jet identification.

8 Results

The observed yields in data, as well as expected yields for the background processes and the signal for several leptoquark masses, after all selection cuts are applied, are shown in table 6. The S_T distribution is used to test for the existence of leptoquarks. Distributions for both channels are shown in figure 2.

At very high S_T , the statistical uncertainties on the various background processes become very poor due to the limited number of MC and (in the case of the multi-jets) data events in the signal region. The sum of the background processes is fitted in the region $350 \text{ GeV} < S_T < 2000 \text{ GeV}$ to an exponential function using a maximum likelihood fit. In this way the distribution is smoothed and a background expectation is provided throughout this S_T region. The fit parameters are varied within their uncertainties to obtain a shape uncertainty. The shape of the S_T distribution is checked for all systematic variations and the variation is found to be significantly smaller than the fit uncertainty in almost all cases. The only exception is for the variation in choice of generator used to model the

	Background	LQ($m=500$ GeV)
Luminosity	–	3.7
Theory	2.8	17
Normalisation factors	9	–
Trigger efficiency	< 0.2	3.3
Muon momentum scale	0.1	0.2
Muon reconstruction efficiency	< 0.1	0.3
Tau energy scale	0.6	1.2
Tau ID efficiency	0.8	5.7
Jet energy scale (nuisance parameter dependent)	0.1 – 2.0	< 0.2
Jet energy resolution	1.5	0.5
b -tagging efficiency	2.7	15

Table 5. The sources of systematic uncertainty in the muon channel and the relative change (in %) in the background and signal yields. The theory term includes uncertainties related to initial- and final-state radiation, PDFs, and multi-parton interactions.

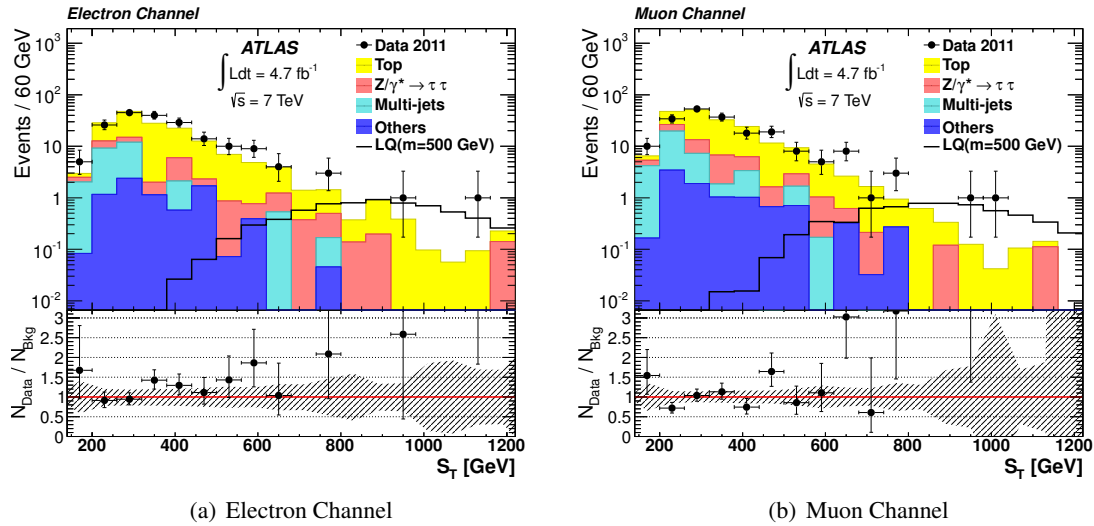


Figure 2. Data and MC comparisons of the S_T variable after applying all cuts in the (a) electron and (b) muon channels. The ratio $N_{\text{Data}}/N_{\text{Background}}$ is also shown, where the red line at unity and hashed band represent the Standard Model expectation and associated statistical and systematic uncertainties. No events with $S_T > 1.2$ TeV were observed in data.

$t\bar{t}$ background process, where the central value lies outside the nominal range (although covers the nominal value within its own statistical uncertainty). Conservatively, the difference between the nominal shape and the alternative shape is taken as a systematic uncertainty and added to the shape uncertainty determined from the nominal fit. The total shape uncertainty is treated as an additional nuisance parameter. Comparisons of the fitted distributions to data are shown in figure 3. Below $S_T = 350$ GeV the background shape is taken from the histogram.

Two alternative models are built to describe background-only and signal+background hypothe-

	Electron channel	Muon channel
$Z/\gamma^* \rightarrow \ell\ell+\text{jets}$	2.1 ± 0.9	1.1 ± 0.5
$Z/\gamma^* \rightarrow \tau\tau+\text{jets}$	21.4 ± 2.2	26.6 ± 2.2
$W+\text{jets}$	5.2 ± 1.2	7.1 ± 1.5
$t\bar{t}$ and single-top	119 ± 11	130 ± 11
Di-boson	1.1 ± 0.2	1.3 ± 0.2
Multi-jets	20^{+13}_{-16}	29 ± 8
Total background	169^{+27}_{-32}	195 ± 18
Data	187	198
$m_{LQ} = 200 \text{ GeV}$	711 ± 22	839 ± 25
$m_{LQ} = 300 \text{ GeV}$	131 ± 3	136 ± 3
$m_{LQ} = 400 \text{ GeV}$	28.7 ± 0.6	28.6 ± 0.6
$m_{LQ} = 500 \text{ GeV}$	7.53 ± 0.15	6.84 ± 0.15
$m_{LQ} = 600 \text{ GeV}$	2.1 ± 0.04	1.87 ± 0.04

Table 6. Yields for data, background and several leptoquark masses in both channels after all cuts are applied. The errors include statistical uncertainties and systematic uncertainties on the background normalisation.

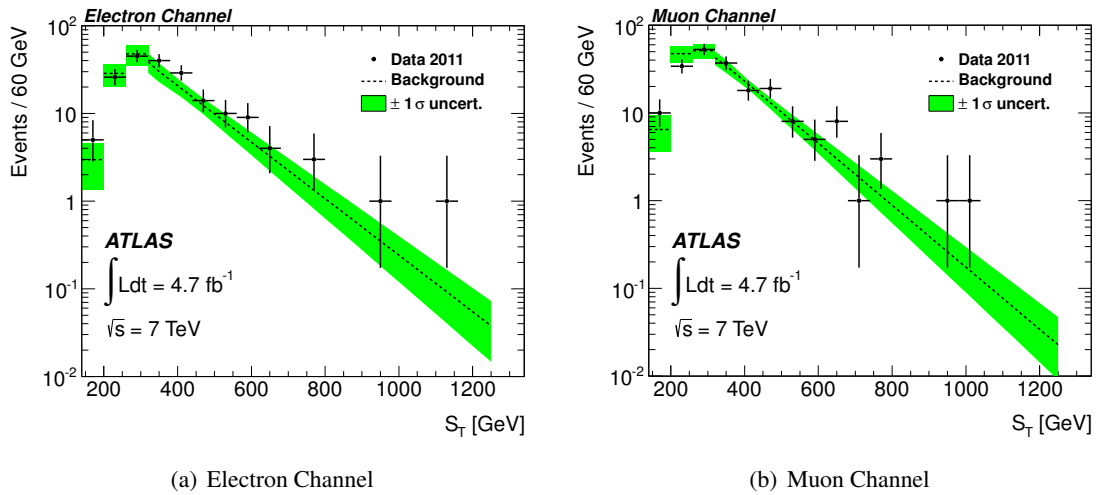
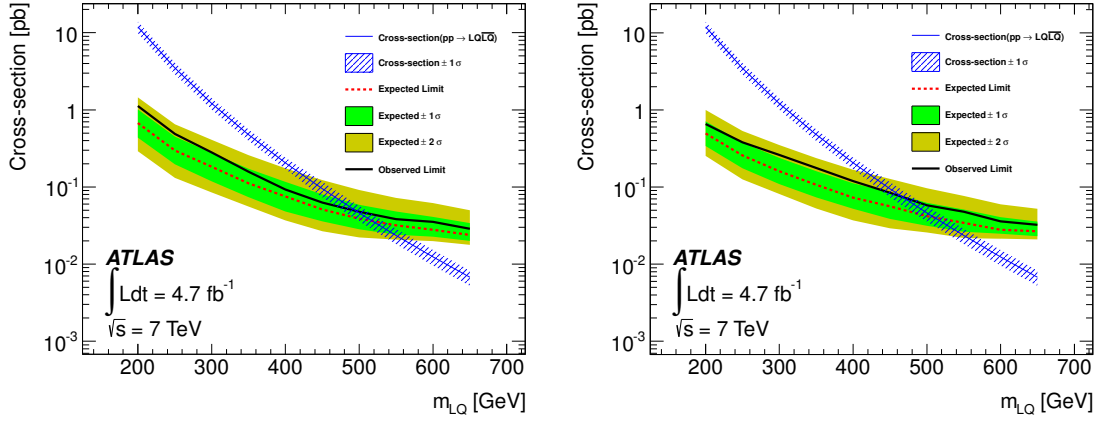


Figure 3. Comparison of the fitted S_T background shape to data in the (a) electron and (b) muon channels. The $\pm 1\sigma$ band represents the uncertainty on the shape of the S_T distribution, obtained by varying the fit parameters within their uncertainties and comparing with the shape of the S_T distribution obtained for each systematic variation. No events with $S_T > 1.2 \text{ TeV}$ were observed in data.

ses. The signal component is calculated separately for each leptoquark mass, thus taking the mass dependence of the S_T distribution into account. For each mass hypothesis, a single ‘signal strength’ parameter (μ) multiplies the expected signal in each bin, where $\mu = 0$ corresponds to the absence of a signal and $\mu = 1$ corresponds to the presence of a signal with nominal strength. The model describes the expected number of signal (s_i) and background (b_i) events in each bin using a Poisson distribution. All systematic uncertainties described in section 7 are assumed to be distributed



(a) Electron Channel

(b) Muon Channel

Figure 4. The expected (dashed) and observed (solid) 95% credibility upper limits on the cross-section as a function of leptoquark mass, in the (a) electron and (b) muon channels. The $1(2) \sigma$ error bands on the expected limit represent all sources of systematic and statistical uncertainty. The expected NLO production cross-section for third generation scalar leptoquarks and its corresponding theoretical uncertainty (hashed band) are also included.

according to a Gaussian function and implemented as multiplicative constraint terms. The correlation of the systematic uncertainties across channels is taken into account. Statistical uncertainties in signal and background histogram bins are also treated as nuisance parameters and assumed to be distributed according to a Poisson function. The statistical analysis of the data employs a binned likelihood function $\mathcal{L}(\mu, \theta)$. The likelihood in each channel is a product over bins in the S_T distributions defined as

$$\mathcal{L}(\mu, \theta) = \prod_{i=\text{bin}} \text{Poisson}(N_i | \mu s_i + b_i), \quad (8.1)$$

where s_i and b_i are the expected number of signal and background events in bin i respectively, and N_i is the observed number of events. Both s_i and b_i depend on nuisance parameters θ . Pseudo-experiments are generated according to background-only and signal+background models to obtain distributions of the test statistic, $\log(\mathcal{L}(\mu, \theta)/\mathcal{L}(0, \theta))$. The CLs method [57] is used to calculate the p-values³. The signal strength parameter is varied iteratively to find the 95% confidence level.

The resulting cross-section limits as a function of leptoquark mass are calculated. It is assumed that $BR(LQ \rightarrow \tau b) = 1.0$. The 95% CL upper bounds on the NLO cross-section for scalar leptoquark pair production as a function of mass are shown for individual channels in figures 4(a) and 4(b). Error bands for the expected limits include all sources of uncertainty. Third generation scalar leptoquarks are observed (expected) to be excluded at 95% confidence level for masses below 498 (523) GeV and 473 (514) GeV in the electron and muon channels respectively by comparing the limits with theoretical predictions of cross-section versus m_{LQ} . The limit is taken using the nominal theoretical calculation for the leptoquark production cross-section at NLO. The uncertainty

³The p-value is the probability of obtaining a test statistic at least as extreme as the one that was actually observed, assuming that the null hypothesis is true

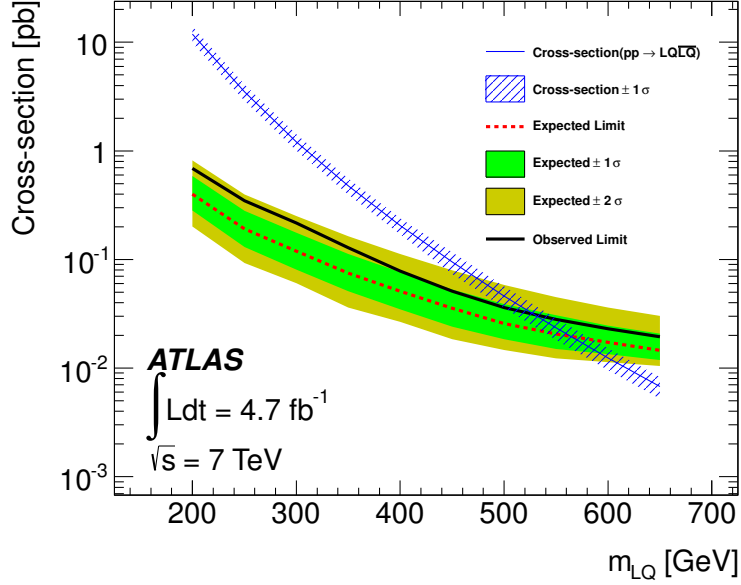


Figure 5. The expected (dashed) and observed (solid) 95% credibility upper limits on the cross-section as a function of leptoquark mass, for the combined result. The $1(2)\sigma$ error bands on the expected limit represent all sources of systematic and statistical uncertainty. The expected NLO production cross-section for third generation scalar leptoquarks and its corresponding theoretical uncertainty (hashed band) are also included.

on the cross-section is also shown. The result when both channels are combined is shown in figure 5. The likelihood for the combined model is defined as the product of likelihood terms for each channel. The data are found to be consistent with the background-only hypothesis and third generation scalar leptoquark production is excluded at 95% confidence level for leptoquark masses up to 534 GeV (the expected limit is 569 GeV).

9 Conclusions

A search for pair production of third generation scalar leptoquarks has been performed with the ATLAS detector at the LHC, using a data sample corresponding to an integrated luminosity of 4.7 fb^{-1} . No significant excess over the SM background expectation is observed in the data. The assumption is made that $BR(LQ \rightarrow \tau b) = 1.0$ and third generation scalar leptoquarks with masses up to $m_{LQ} < 534\text{ GeV}$ are excluded at 95% CL. The cross-section for leptoquark pair-production increases with centre-of-mass collision energy. At $\sqrt{s} = 8\text{ TeV}$ the production rate for leptoquarks with $m_{LQ} = 700\text{ GeV}$ is enhanced by a factor of two, providing scope for setting stronger limits using data from the 2012 LHC run. Meanwhile, this result is the most stringent limit arising from direct searches for third generation scalar leptoquarks to-date.

10 Acknowledgements

We thank CERN for the very successful operation of the LHC, as well as the support staff from our institutions without whom ATLAS could not be operated efficiently.

We acknowledge the support of ANPCyT, Argentina; YerPhI, Armenia; ARC, Australia; BMWF and FWF, Austria; ANAS, Azerbaijan; SSTC, Belarus; CNPq and FAPESP, Brazil; NSERC, NRC and CFI, Canada; CERN; CONICYT, Chile; CAS, MOST and NSFC, China; COLCIENCIAS, Colombia; MSMT CR, MPO CR and VSC CR, Czech Republic; DNRF, DNSRC and Lundbeck Foundation, Denmark; EPLANET, ERC and NSRF, European Union; IN2P3-CNRS, CEA-DSM/IRFU, France; GNSF, Georgia; BMBF, DFG, HGF, MPG and AvH Foundation, Germany; GSRT and NSRF, Greece; ISF, MINERVA, GIF, DIP and Benoziyo Center, Israel; INFN, Italy; MEXT and JSPS, Japan; CNRST, Morocco; FOM and NWO, Netherlands; BRF and RCN, Norway; MNiSW, Poland; GRICES and FCT, Portugal; MERYS (MECTS), Romania; MES of Russia and ROSATOM, Russian Federation; JINR; MSTD, Serbia; MSSR, Slovakia; ARRS and MIZŠ, Slovenia; DST/NRF, South Africa; MICINN, Spain; SRC and Wallenberg Foundation, Sweden; SER, SNSF and Cantons of Bern and Geneva, Switzerland; NSC, Taiwan; TAEK, Turkey; STFC, the Royal Society and Leverhulme Trust, United Kingdom; DOE and NSF, United States of America.

The crucial computing support from all WLCG partners is acknowledged gratefully, in particular from CERN and the ATLAS Tier-1 facilities at TRIUMF (Canada), NDGF (Denmark, Norway, Sweden), CC-IN2P3 (France), KIT/GridKA (Germany), INFN-CNAF (Italy), NL-T1 (Netherlands), PIC (Spain), ASGC (Taiwan), RAL (UK) and BNL (USA) and in the Tier-2 facilities worldwide.

References

- [1] S. K. Dimopoulos and L. Susskind. Mass without scalars. *Nucl. Phys. B.*, 155(1):237–252, 1979.
- [2] S. Dimopoulos. Technicoloured signatures. *Nucl. Phys. B.*, 168:69–92, 1980.
- [3] E. J. Eichten and K. Lane. Dynamical breaking of weak interaction symmetries. *Phys. Lett. B.*, 90(1,2):125–130, 1980.
- [4] V. D. Angelopoulos, J. R. Ellis, H. Kowalski, et al. Search for new quarks suggested by the superstring. *Nucl. Phys. B.*, 292:59–92, 1986.
- [5] W. Buchmüller and D. Wyler. Constraints on SU(5)-type leptoquarks. *Phys. Lett. B.*, 177:377–382, 1986.
- [6] J. C. Pati and A. Salam. Lepton number as the fourth ‘colour’. *Phys. Rev. D.*, 10:275–289, 1974. *Erratum ibid.* D11.703, 1975.
- [7] H. Georgi and S.L. Glashow. Unity of All Elementary Particle Forces. *Phys. Rev. Lett.*, 32:438–441, 1974.
- [8] S. Kovalenko and I. Schmidt. Proton stability in leptoquark models. *Phys. Lett. B.*, 562:104–108, 2003. arXiv:0210187 [hep-ph].
- [9] W. Buchmüller, R. Rückl, and D. Wyler. Leptoquarks in lepton-quark collisions. *Phys. Lett. B.*, 191:442–448, 1986. *Erratum ibid.* B448:320, 1999.
- [10] CMS Collaboration. Search for pair production of third-generation leptoquarks and top squarks in pp collisions at $\sqrt{s} = 7$ TeV. *Phys. Rev. Lett.*, 110(081801), 2013. arXiv:1210.5629 [hep-ex].
- [11] D0 Collaboration. Search for third generation scalar leptoquarks decaying into τb . *Phys. Rev. Lett.*, 101:241802, 2008. arXiv:0806.3527 [hep-ex].

- [12] CDF Collaboration. Search for Pair Production of Scalar Top Quarks Decaying to a τ Lepton and a b Quark in $p\bar{p}$ Collisions at $\sqrt{s} = 1.96$ TeV. *Phys. Rev. Lett.*, 101:071802, 2008. arXiv:0802.3887 [hep-ex].
- [13] CMS Collaboration. Search for pair production of first- and second-generation scalar leptoquarks in pp collisions at $\sqrt{s} = 7$ TeV. *Phys. Rev. D.*, 86:052013, 2012. arXiv:1207.5406 [hep-ex].
- [14] ATLAS Collaboration. Search for first generation scalar leptoquarks in pp collisions at $\sqrt{s} = 7$ TeV with the ATLAS detector. *Phys. Lett. B.*, 709:158–176, 2012. *Erratum ibid.* 711:442–455, 2012. arXiv:1112.4828 [hep-ex].
- [15] ATLAS Collaboration. Search for second generation scalar leptoquarks in pp collisions at $\sqrt{s} = 7$ TeV with the ATLAS detector. *Eur. Phys. J. C.*, 72:2151, 2012. arXiv:1203.3172 [hep-ex].
- [16] ATLAS Collaboration. The ATLAS Experiment at the CERN Large Hadron Collider. *J. Instrum.*, 3(S08003), 2008.
- [17] T. Sjöstrand, S. Mrenna, and P. Z. Skands. PYTHIA 6.4 Physics and Manual. *J. High Energy Phys.*, 05:026, 2006. arXiv:0603175 [hep-ph].
- [18] R. Field. Physics at the Tevatron. *Acta Physica Polonica B.*, 39:2611–2671, 2008.
- [19] J. Pumplin, D.R. Stump, J. Huston, et al. New generation of parton distributions with uncertainties from global QCD analysis. *J. High Energy Phys.*, 0207:012, 2002. arXiv:0201195 [hep-ph].
- [20] A Belyaev, C Leroy, R Mehdiyev, et al. Leptoquark Single and Pair production at LHC with CalcHEP/CompHEP in the complete model. *J. High Energy Phys.*, 09(005), 2005. arXiv:0502067 [hep-ph].
- [21] M. Krämer, T. Plehn, M. Spira, et al. Pair production of scalar leptoquarks at the CERN LHC. *Phys. Rev. D.*, 71:057503, 2005. arXiv:0411038 [hep-ph].
- [22] M. L. Mangano, M. Moretti, F. Piccinini, et al. ALPGEN, a generator for hard multiparton processes in hadronic collisions. *J. High Energy Phys.*, 07:001, 2003. arXiv:0206293 [hep-ph].
- [23] J. Alwall, S. Hoeche, F. Krauss, et al. Comparative study of various algorithms for the merging of parton showers and matrix elements in hadronic collisions. *Eur. Phys. J.*, C53:473–500, 2008. arXiv:0706.2569 [hep-ph].
- [24] G. Corcella, I. G. Knowles, G. Marchesini, et al. HERWIG 6: An event generator for hadron emission reactions with interfering gluons (including supersymmetric processes). *J. High Energy Phys.*, 0101:010, 2001. arXiv:0011363 [hep-ph].
- [25] J. M. Butterworth, J. R. Forshaw, and M. H. Seymour. Multiparton interactions in photoproduction at HERA. *Z. Phys.*, C72:637–646, 1996. arXiv:9601371 [hep-ex].
- [26] A. Sherstnev and R.S. Thorne. Parton Distributions for LO Generators. *Eur. Phys. J.*, C55:553–575, 2008. arXiv:0711.2473 [hep-ph].
- [27] S. Frixione, F. Stoeckli, P. Torrielli, et al. The MC@NLO 4.0 Event Generator. 2010. CAVENDISH-HEP-10-12. CERN-PH-TH-2010-216. IPPP-10-62. DCPT-10-124. arXiv:1010.0819[hep-ph].
- [28] S. Frixione and B. R. Webber. Matching NLO QCD computations and parton shower simulations. *J. High Energy Phys.*, 06:029, 2002. hep-ph/0204244.
- [29] S. Frixione, P. Nason, and B. R. Webber. Matching NLO QCD and parton showers in heavy flavour production. *J. High Energy Phys.*, 08:007, 2003. hep-ph/0305252.

- [30] S. Frixione, E. Laenen, P. Motylinski, et al. Single-top hadroproduction in association with a W boson. *J. High Energy Phys.*, 07:029, 2008. arXiv:0805.3067.
- [31] H. Lai, M. Guzzi, J. Huston, et al. New parton distributions for collider physics. *Phys. Rev.*, D82:074024, 2010. arXiv:1007.2241 [hep-ph].
- [32] P. B. Kersevan and E. Richter-Was. The Monte Carlo event generator AcerMC version 2.0 with Interfaces to PYTHIA 6.2 and HERWIG 6.5. 2004. TPJU-2004-6.
- [33] S. Jadach, Z. Was, R. Decker, et al. The tau decay library TAUOLA, Version 2.4. *Comput. Phys. Commun.*, 76:361–380, 1993.
- [34] E. Barberio and Z. Was. PHOTOS: a universal Monte Carlo for QED radiative corrections. Version 2.0. *Comput. Phys. Commun.*, 79:291–308, 1994.
- [35] M Aliev, H Lacker, U Langenfeld, et al. – HATHOR – HAdronic Top and Heavy quarks crOss section calculatoR. *Comput. Phys. Commun.*, 182:1034–1046, 2011. arXiv:1007.1327 [hep-ph].
- [36] ATLAS Collaboration. ATLAS Simulation Infrastructure. *Eur. Phys. J. C.*, 70:823–874, 2010. arXiv:1005.4568 [physics.ins-det].
- [37] S. Agostinelli et al. GEANT4: A Simulation Toolkit. *Nucl. Instrum. Meth.*, A506:250–303, 2003.
- [38] ATLAS Collaboration. Expected electron performance in the ATLAS experiment. April 2011. ATL-PHYS-PUB-2011-006. <https://cdsweb.cern.ch/record/1345327>.
- [39] ATLAS Collaboration. Muon reconstruction efficiency in reprocessed 2010 lhq proton-proton collision data recorded with the atlas detector. 2011. ATLAS-CONF-2011-063. <http://cdsweb.cern.ch/record/1345743>.
- [40] M. Cacciari, G. P. Salam, and G. Soyez. The anti- k_t jet clustering algorithm. *J. High Energy Phys.*, 04:063, 2008. arXiv:0802.1189 [hep-ph].
- [41] W Lampl, S Laplace, D Lelas, et al. Calorimeter Clustering Algorithms: Description and Performance. Apr 2008. ATL-LARG-PUB-2008-002. <http://cdsweb.cern.ch/record/1099735>.
- [42] ATLAS Collaboration. In situ jet pseudorapidity intercalibration of the ATLAS detector using dijet events in $\sqrt{s}=7$ TeV proton-proton 2011 data. Aug 2012. ATLAS-CONF-2012-124. <http://cdsweb.cern.ch/record/1474490>.
- [43] ATLAS Collaboration. Commissioning of the ATLAS high-performance b -tagging algorithms in the 7 TeV collision data. Jul 2011. ATLAS-CONF-2011-102. <http://cdsweb.cern.ch/record/1369219>.
- [44] ATLAS Collaboration. Performance of the Reconstruction and Identification of Hadronic Tau Decays with ATLAS. Nov 2011. ATLAS-CONF-2011-152. <http://cdsweb.cern.ch/record/1398195>.
- [45] B. P. Roe, H. Yang, J. Zhu, et al. Boosted decision trees, an alternative to artificial neural networks. *Nucl. Instrum. Meth.*, A543:577–584, 2005. arXiv:0408124 [physics.data-an].
- [46] ATLAS Collaboration. Selection of jets produced in proton-proton collisions with the ATLAS detector using 2011 data. Mar 2012. ATLAS-CONF-2012-020. <https://cdsweb.cern.ch/record/1430034>.
- [47] ATLAS Collaboration. Measurement of the Mis-identification Probability of τ Leptons from Hadronic Jets and from Electrons. Aug 2011. ATLAS-CONF-2011-113. <http://cdsweb.cern.ch/record/1375550>.
- [48] ATLAS Collaboration. Performance of the ATLAS Electron and Photon Trigger in $p-p$ Collisions at $\sqrt{s} = 7$ TeV in 2011. May 2012. ATLAS-CONF-2012-048. <https://cdsweb.cern.ch/record/1450089>.

- [49] ATLAS Collaboration. Performance of the ATLAS muon trigger in 2011. Jul 2012. ATLAS-CONF-2012-099. <https://cdsweb.cern.ch/record/1462601>.
- [50] ATLAS Collaboration. Determination of the tau energy scale and the associated systematic uncertainty in proton-proton collisions at $\sqrt{s} = 7$ TeV with the ATLAS detector at the LHC in 2011. Jun 2012. ATLAS-CONF-2012-054. <http://cdsweb.cern.ch/record/1453781>.
- [51] ATLAS Collaboration. Luminosity Determination in pp Collisions at $\sqrt{s} = 7$ TeV using the ATLAS Detector in 2011. Aug 2011. ATLAS-CONF-2011-116. <https://cdsweb.cern.ch/record/1376384>.
- [52] P. Nason. A New method for combining NLO QCD with shower Monte Carlo algorithms. *J. High Energy Phys.*, 0411:040, 2004. arXiv:0409146 [hep-ph].
- [53] S. Frixione, P. Nason, and C. Oleari. Matching NLO QCD computations with Parton Shower simulations: the POWHEG method. *J. High Energy Phys.*, 0711:070, 2007. arXiv:0709.2092 [hep-ph].
- [54] ATLAS Collaboration. Expected Performance of the ATLAS Experiment - Detector, Trigger and Physics. 2009. CERN-OPEN-2008-020. arXiv:0901.0512 [hep-ex].
- [55] S. Badger, J. M. Campbell, and R.K. Ellis. QCD corrections to the hadronic production of a heavy quark pair and a W-boson including decay correlations. *J. High Energy Phys.*, 1103:027, 2011. arXiv:1011.6647 [hep-ph].
- [56] J. M. Campbell, R. K. Ellis, F. Maltoni, et al. Production of a Z boson and two jets with one heavy-quark tag. *Phys. Rev. D.*, 73:054007, 2006. *Erratum ibid.* D77:019903, 2008. arXiv:0510362 [hep-ph].
- [57] A. L. Read. Presentation of search results: The CL(s) technique. *J. Phys.*, G28:2693–2704, 2002.

The ATLAS Collaboration

G. Aad⁴⁸, T. Abajyan²¹, B. Abbott¹¹¹, J. Abdallah¹², S. Abdel Khalek¹¹⁵, A.A. Abdelalim⁴⁹, O. Abdinov¹¹, R. Aben¹⁰⁵, B. Abi¹¹², M. Abolins⁸⁸, O.S. AbouZeid¹⁵⁸, H. Abramowicz¹⁵³, H. Abreu¹³⁶, B.S. Acharya^{164a,164b,a}, L. Adamczyk³⁸, D.L. Adams²⁵, T.N. Addy⁵⁶, J. Adelman¹⁷⁶, S. Adomeit⁹⁸, P. Adragna⁷⁵, T. Adye¹²⁹, S. Aefsky²³, J.A. Aguilar-Saavedra^{124b,b}, M. Agustoni¹⁷, M. Aharrouche⁸¹, S.P. Ahlen²², F. Ahles⁴⁸, A. Ahmad¹⁴⁸, M. Ahsan⁴¹, G. Aielli^{133a,133b}, T.P.A. Åkesson⁷⁹, G. Akimoto¹⁵⁵, A.V. Akimov⁹⁴, M.A. Alam⁷⁶, J. Albert¹⁶⁹, S. Albrand⁵⁵, M. Aleksa³⁰, I.N. Aleksandrov⁶⁴, F. Alessandria^{89a}, C. Alexa^{26a}, G. Alexander¹⁵³, G. Alexandre⁴⁹, T. Alexopoulos¹⁰, M. Alhroob^{164a,164c}, M. Aliev¹⁶, G. Alimonti^{89a}, J. Alison¹²⁰, B.M.M. Allbrooke¹⁸, P.P. Allport⁷³, S.E. Allwood-Spiers⁵³, J. Almond⁸², A. Aloisio^{102a,102b}, R. Alon¹⁷², A. Alonso⁷⁹, F. Alonso⁷⁰, A. Altheimer³⁵, B. Alvarez Gonzalez⁸⁸, M.G. Alviggi^{102a,102b}, K. Amako⁶⁵, C. Amelung²³, V.V. Ammosov^{128,*}, S.P. Amor Dos Santos^{124a}, A. Amorim^{124a,c}, N. Amram¹⁵³, C. Anastopoulos³⁰, L.S. Ancu¹⁷, N. Andari¹¹⁵, T. Andeen³⁵, C.F. Anders^{58b}, G. Anders^{58a}, K.J. Anderson³¹, A. Andreazza^{89a,89b}, V. Andrei^{58a}, M.-L. Andrieux⁵⁵, X.S. Anduaga⁷⁰, S. Angelidakis⁹, P. Anger⁴⁴, A. Angerami³⁵, F. Anghinolfi³⁰, A. Anisenkov¹⁰⁷, N. Anjos^{124a}, A. Annovi⁴⁷, A. Antonaki⁹, M. Antonelli⁴⁷, A. Antonov⁹⁶, J. Antos^{144b}, F. Anulli^{132a}, M. Aoki¹⁰¹, S. Aoun⁸³, L. Aperio Bella⁵, R. Apolle^{118,d}, G. Arabidze⁸⁸, I. Aracena¹⁴³, Y. Arai⁶⁵, A.T.H. Arce⁴⁵, S. Arfaoui¹⁴⁸, J.-F. Arguin⁹³, S. Argyropoulos⁴², E. Arik^{19a,*}, M. Arik^{19a}, A.J. Armbruster⁸⁷, O. Arnaez⁸¹, V. Arnal⁸⁰, A. Artamonov⁹⁵, G. Artoni^{132a,132b}, D. Arutinov²¹, S. Asai¹⁵⁵, S. Ask²⁸, B. Åsman^{146a,146b}, L. Asquith⁶, K. Assamagan^{25,e}, A. Astbury¹⁶⁹, M. Atkinson¹⁶⁵, B. Aubert⁵, E. Auge¹¹⁵, K. Augsten¹²⁶, M. Auresseau^{145a}, G. Avolio³⁰, D. Axen¹⁶⁸, G. Azuelos^{93,f}, Y. Azuma¹⁵⁵, M.A. Baak³⁰, G. Baccaglioni^{89a}, C. Bacci^{134a,134b}, A.M. Bach¹⁵, H. Bachacou¹³⁶, K. Bachas¹⁵⁴, M. Backes⁴⁹, M. Backhaus²¹, J. Backus Mayes¹⁴³, E. Badescu^{26a}, P. Bagnaia^{132a,132b}, S. Bahinipati³, Y. Bai^{33a}, D.C. Bailey¹⁵⁸, T. Bain³⁵, J.T. Baines¹²⁹, O.K. Baker¹⁷⁶, M.D. Baker²⁵, S. Baker⁷⁷, P. Balek¹²⁷, E. Banas³⁹, P. Banerjee⁹³, Sw. Banerjee¹⁷³, D. Banfi³⁰, A. Bangert¹⁵⁰, V. Bansal¹⁶⁹, H.S. Bansil¹⁸, L. Barak¹⁷², S.P. Baranov⁹⁴, A. Barbaro Galtieri¹⁵, T. Barber⁴⁸, E.L. Barberio⁸⁶, D. Barberis^{50a,50b}, M. Barbero²¹, D.Y. Bardin⁶⁴, T. Barillari⁹⁹, M. Barisonzi¹⁷⁵, T. Barklow¹⁴³, N. Barlow²⁸, B.M. Barnett¹²⁹, R.M. Barnett¹⁵, A. Baroncelli^{134a}, G. Barone⁴⁹, A.J. Barr¹¹⁸, F. Barreiro⁸⁰, J. Barreiro Guimarães da Costa⁵⁷, R. Bartoldus¹⁴³, A.E. Barton⁷¹, V. Bartsch¹⁴⁹, A. Basye¹⁶⁵, R.L. Bates⁵³, L. Batkova^{144a}, J.R. Batley²⁸, A. Battaglia¹⁷, M. Battistin³⁰, F. Bauer¹³⁶, H.S. Bawa^{143,g}, S. Beale⁹⁸, T. Beau⁷⁸, P.H. Beauchemin¹⁶¹, R. Beccherle^{50a}, P. Bechtel²¹, H.P. Beck¹⁷, K. Becker¹⁷⁵, S. Becker⁹⁸, M. Beckingham¹³⁸, K.H. Becks¹⁷⁵, A.J. Beddall^{19c}, A. Beddall^{19c}, S. Bedikian¹⁷⁶, V.A. Bednyakov⁶⁴, C.P. Bee⁸³, L.J. Beamster¹⁰⁵, M. Bege²⁵, S. Behar Harpaz¹⁵², P.K. Behera⁶², M. Beimforde⁹⁹, C. Belanger-Champagne⁸⁵, P.J. Bell⁴⁹, W.H. Bell⁴⁹, G. Bella¹⁵³, L. Bellagamba^{20a}, M. Bellomo³⁰, A. Belloni⁵⁷, O. Beloborodova^{107,h}, K. Belotskiy⁹⁶, O. Beltramello³⁰, O. Benary¹⁵³, D. Bencheikroun^{135a}, K. Bendtz^{146a,146b}, N. Benekos¹⁶⁵, Y. Benhammou¹⁵³, E. Benhar Nocchioli⁴⁹, J.A. Benitez Garcia^{159b}, D.P. Benjamin⁴⁵, M. Benoit¹¹⁵, J.R. Bensinger²³, K. Benslama¹³⁰, S. Bentvelsen¹⁰⁵, D. Berge³⁰, E. Bergeas Kuutmann⁴², N. Berger⁵, F. Berghaus¹⁶⁹, E. Berglund¹⁰⁵, J. Beringer¹⁵, P. Bernat⁷⁷, R. Bernhard⁴⁸, C. Bernius²⁵, T. Berry⁷⁶, C. Bertella⁸³, A. Bertin^{20a,20b}, F. Bertolucci^{122a,122b},

M.I. Besana^{89a,89b}, G.J. Besjes¹⁰⁴, N. Besson¹³⁶, S. Bethke⁹⁹, W. Bhimji⁴⁶, R.M. Bianchi³⁰,
L. Bianchini²³, M. Bianco^{72a,72b}, O. Biebel⁹⁸, S.P. Bieniek⁷⁷, K. Bierwagen⁵⁴, J. Biesiada¹⁵,
M. Biglietti^{134a}, H. Bilokon⁴⁷, M. Bindi^{20a,20b}, S. Binet¹¹⁵, A. Bingul^{19c}, C. Bini^{132a,132b},
C. Biscarat¹⁷⁸, B. Bittner⁹⁹, C.W. Black¹⁵⁰, K.M. Black²², R.E. Blair⁶, J.-B. Blanchard¹³⁶,
T. Blazek^{144a}, I. Bloch⁴², C. Blocker²³, J. Blocki³⁹, A. Blondel⁴⁹, W. Blum⁸¹, U. Blumenschein⁵⁴,
G.J. Bobbink¹⁰⁵, V.S. Bobrovnikov¹⁰⁷, S.S. Bocchetta⁷⁹, A. Bocci⁴⁵, C.R. Boddy¹¹⁸,
M. Boehler⁴⁸, J. Boek¹⁷⁵, T.T. Boek¹⁷⁵, N. Boelaert³⁶, J.A. Bogaerts³⁰, A. Bogdanchikov¹⁰⁷,
A. Bogouch^{90,*}, C. Bohm^{146a}, J. Bohm¹²⁵, V. Boisvert⁷⁶, T. Bold³⁸, V. Boldea^{26a}, N.M. Bolnet¹³⁶,
M. Bomben⁷⁸, M. Bona⁷⁵, M. Boonekamp¹³⁶, S. Bordoni⁷⁸, C. Borer¹⁷, A. Borisov¹²⁸,
G. Borissov⁷¹, I. Borjanovic^{13a}, M. Borri⁸², S. Borroni⁸⁷, J. Bortfeldt⁹⁸, V. Bortolotto^{134a,134b},
K. Bos¹⁰⁵, D. Boscherini^{20a}, M. Bosman¹², H. Boterenbrood¹⁰⁵, J. Bouchami⁹³, J. Boudreau¹²³,
E.V. Bouhova-Thacker⁷¹, D. Boumediene³⁴, C. Bourdarios¹¹⁵, N. Bousson⁸³, A. Boveia³¹,
J. Boyd³⁰, I.R. Boyko⁶⁴, I. Bozovic-Jelisavcic^{13b}, J. Bracinik¹⁸, P. Branchini^{134a}, A. Brandt⁸,
G. Brandt¹¹⁸, O. Brandt⁵⁴, U. Bratzler¹⁵⁶, B. Brau⁸⁴, J.E. Brau¹¹⁴, H.M. Braun^{175,*},
S.F. Brazzale^{164a,164c}, B. Brelrier¹⁵⁸, J. Bremer³⁰, K. Brendlinger¹²⁰, R. Brenner¹⁶⁶, S. Bressler¹⁷²,
D. Britton⁵³, F.M. Brochu²⁸, I. Brock²¹, R. Brock⁸⁸, F. Broggi^{89a}, C. Bromberg⁸⁸, J. Bronner⁹⁹,
G. Brooijmans³⁵, T. Brooks⁷⁶, W.K. Brooks^{32b}, G. Brown⁸², P.A. Bruckman de Renstrom³⁹,
D. Bruncko^{144b}, R. Bruneliere⁴⁸, S. Brunet⁶⁰, A. Bruni^{20a}, G. Bruni^{20a}, M. Bruschi^{20a},
L. Bryngemark⁷⁹, T. Buanes¹⁴, Q. Buat⁵⁵, F. Bucci⁴⁹, J. Buchanan¹¹⁸, P. Buchholz¹⁴¹,
R.M. Buckingham¹¹⁸, A.G. Buckley⁴⁶, S.I. Buda^{26a}, I.A. Budagov⁶⁴, B. Budick¹⁰⁸, V. Buischer⁸¹,
L. Bugge¹¹⁷, O. Bulekov⁹⁶, A.C. Bundock⁷³, M. Bunse⁴³, T. Buran¹¹⁷, H. Burckhart³⁰,
S. Burdin⁷³, T. Burgess¹⁴, S. Burke¹²⁹, E. Busato³⁴, P. Bussey⁵³, C.P. Buszello¹⁶⁶, B. Butler¹⁴³,
J.M. Butler²², C.M. Buttar⁵³, J.M. Butterworth⁷⁷, W. Buttinger²⁸, M. Byszewski³⁰,
S. Cabrera Urbán¹⁶⁷, D. Caforio^{20a,20b}, O. Cakir^{4a}, P. Calafiura¹⁵, G. Calderini⁷⁸, P. Calfayan⁹⁸,
R. Calkins¹⁰⁶, L.P. Caloba^{24a}, R. Caloi^{132a,132b}, D. Calvet³⁴, S. Calvet³⁴, R. Camacho Toro³⁴,
P. Camarri^{133a,133b}, D. Cameron¹¹⁷, L.M. Caminada¹⁵, R. Caminal Armadans¹², S. Campana³⁰,
M. Campanelli⁷⁷, V. Canale^{102a,102b}, F. Canelli³¹, A. Canepa^{159a}, J. Cantero⁸⁰, R. Cantrill⁷⁶,
L. Capasso^{102a,102b}, M.D.M. Capeans Garrido³⁰, I. Caprini^{26a}, M. Caprini^{26a}, D. Capriotti⁹⁹,
M. Capua^{37a,37b}, R. Caputo⁸¹, R. Cardarelli^{133a}, T. Carli³⁰, G. Carlino^{102a}, L. Carminati^{89a,89b},
B. Caron⁸⁵, S. Caron¹⁰⁴, E. Carquin^{32b}, G.D. Carrillo-Montoya^{145b}, A.A. Carter⁷⁵, J.R. Carter²⁸,
J. Carvalho^{124a,i}, D. Casadei¹⁰⁸, M.P. Casado¹², M. Cascella^{122a,122b}, C. Caso^{50a,50b,*},
A.M. Castaneda Hernandez^{173,j}, E. Castaneda-Miranda¹⁷³, V. Castillo Gimenez¹⁶⁷,
N.F. Castro^{124a}, G. Cataldi^{72a}, P. Catastini⁵⁷, A. Catinaccio³⁰, J.R. Catmore³⁰, A. Cattai³⁰,
G. Cattani^{133a,133b}, S. Caughron⁸⁸, V. Cavaliere¹⁶⁵, P. Cavalleri⁷⁸, D. Cavalli^{89a},
M. Cavalli-Sforza¹², V. Cavalinni^{122a,122b}, F. Ceradini^{134a,134b}, A.S. Cerqueira^{24b}, A. Cerri¹⁵,
L. Cerrito⁷⁵, F. Cerutti¹⁵, S.A. Cetin^{19b}, A. Chafaq^{135a}, D. Chakraborty¹⁰⁶, I. Chalupkova¹²⁷,
K. Chan³, P. Chang¹⁶⁵, B. Chapleau⁸⁵, J.D. Chapman²⁸, J.W. Chapman⁸⁷, D.G. Charlton¹⁸,
V. Chavda⁸², C.A. Chavez Barajas³⁰, S. Cheatham⁸⁵, S. Chekanov⁶, S.V. Chekulaev^{159a},
G.A. Chelkov⁶⁴, M.A. Chelstowska¹⁰⁴, C. Chen⁶³, H. Chen²⁵, S. Chen^{33c}, X. Chen¹⁷³, Y. Chen³⁵,
Y. Cheng³¹, A. Cheplakov⁶⁴, R. Cherkaoui El Moursli^{135e}, V. Chernyatin²⁵, E. Cheu⁷,
S.L. Cheung¹⁵⁸, L. Chevalier¹³⁶, G. Chiefari^{102a,102b}, L. Chikovani^{51a,*}, J.T. Childers³⁰,
A. Chilingarov⁷¹, G. Chiodini^{72a}, A.S. Chisholm¹⁸, R.T. Chislett⁷⁷, A. Chitan^{26a}, M.V. Chizhov⁶⁴,
G. Choudalakis³¹, S. Chouridou¹³⁷, I.A. Christidi⁷⁷, A. Christov⁴⁸, D. Chromek-Burckhart³⁰,

M.L. Chu¹⁵¹, J. Chudoba¹²⁵, G. Ciapetti^{132a,132b}, A.K. Ciftci^{4a}, R. Ciftci^{4a}, D. Cinca³⁴,
 V. Cindro⁷⁴, A. Ciocio¹⁵, M. Cirilli⁸⁷, P. Cirkovic^{13b}, Z.H. Citron¹⁷², M. Citterio^{89a},
 M. Ciubancan^{26a}, A. Clark⁴⁹, P.J. Clark⁴⁶, R.N. Clarke¹⁵, W. Cleland¹²³, J.C. Clemens⁸³,
 B. Clement⁵⁵, C. Clement^{146a,146b}, Y. Coadou⁸³, M. Cobal^{164a,164c}, A. Coccaro¹³⁸, J. Cochran⁶³,
 L. Coffey²³, J.G. Cogan¹⁴³, J. Coggeshall¹⁶⁵, J. Colas⁵, S. Cole¹⁰⁶, A.P. Colijn¹⁰⁵, N.J. Collins¹⁸,
 C. Collins-Tooth⁵³, J. Collot⁵⁵, T. Colombo^{119a,119b}, G. Colon⁸⁴, G. Compostella⁹⁹,
 P. Conde Muiño^{124a}, E. Coniavitis¹⁶⁶, M.C. Conidi¹², S.M. Consonni^{89a,89b}, V. Consorti⁴⁸,
 S. Constantinescu^{26a}, C. Conta^{119a,119b}, G. Conti⁵⁷, F. Conventi^{102a,k}, M. Cooke¹⁵, B.D. Cooper⁷⁷,
 A.M. Cooper-Sarkar¹¹⁸, K. Copic¹⁵, T. Cornelissen¹⁷⁵, M. Corradi^{20a}, F. Corriveau^{85,l},
 A. Cortes-Gonzalez¹⁶⁵, G. Cortiana⁹⁹, G. Costa^{89a}, M.J. Costa¹⁶⁷, D. Costanzo¹³⁹, D. Côté³⁰,
 L. Courneyea¹⁶⁹, G. Cowan⁷⁶, B.E. Cox⁸², K. Cranmer¹⁰⁸, F. Crescioli⁷⁸, M. Cristinziani²¹,
 G. Crosetti^{37a,37b}, S. Crépe-Renaudin⁵⁵, C.-M. Cuciuc^{26a}, C. Cuenca Almenar¹⁷⁶,
 T. Cuhadar Donszelmann¹³⁹, J. Cummings¹⁷⁶, M. Curatolo⁴⁷, C.J. Curtis¹⁸, C. Cuthbert¹⁵⁰,
 P. Cwetanski⁶⁰, H. Czirr¹⁴¹, P. Czodrowski⁴⁴, Z. Czyczula¹⁷⁶, S. D'Auria⁵³, M. D'Onofrio⁷³,
 A. D'Orazio^{132a,132b}, M.J. Da Cunha Sargedas De Sousa^{124a}, C. Da Via⁸², W. Dabrowski³⁸,
 A. Dafinca¹¹⁸, T. Dai⁸⁷, F. Dallaire⁹³, C. Dallapiccola⁸⁴, M. Dam³⁶, M. Dameri^{50a,50b},
 D.S. Damiani¹³⁷, H.O. Danielsson³⁰, V. Dao⁴⁹, G. Darbo^{50a}, G.L. Darlea^{26b}, J.A. Dassoulas⁴²,
 W. Davey²¹, T. Davidek¹²⁷, N. Davidson⁸⁶, R. Davidson⁷¹, E. Davies^{118,d}, M. Davies⁹³,
 O. Davignon⁷⁸, A.R. Davison⁷⁷, Y. Davygora^{58a}, E. Dawe¹⁴², I. Dawson¹³⁹,
 R.K. Daya-Ishmukhametova²³, K. De⁸, R. de Asmundis^{102a}, S. De Castro^{20a,20b}, S. De Cecco⁷⁸,
 J. de Graat⁹⁸, N. De Groot¹⁰⁴, P. de Jong¹⁰⁵, C. De La Taille¹¹⁵, H. De la Torre⁸⁰, F. De Lorenzi⁶³,
 L. de Mora⁷¹, L. De Nooij¹⁰⁵, D. De Pedis^{132a}, A. De Salvo^{132a}, U. De Sanctis^{164a,164c},
 A. De Santo¹⁴⁹, J.B. De Vivie De Regie¹¹⁵, G. De Zorzi^{132a,132b}, W.J. Dearnaley⁷¹, R. Debbes²⁵,
 C. Debenedetti⁴⁶, B. Dechenaux⁵⁵, D.V. Dedovich⁶⁴, J. Degenhardt¹²⁰, J. Del Peso⁸⁰,
 T. Del Prete^{122a,122b}, T. Delemontex⁵⁵, M. Deliyergiyev⁷⁴, A. Dell'Acqua³⁰, L. Dell'Asta²²,
 M. Della Pietra^{102a,k}, D. della Volpe^{102a,102b}, M. Delmastro⁵, P.A. Delsart⁵⁵, C. Deluca¹⁰⁵,
 S. Demers¹⁷⁶, M. Demichev⁶⁴, B. Demirkoz^{12,m}, S.P. Denisov¹²⁸, D. Derendarz³⁹,
 J.E. Derkaoui^{135d}, F. Derue⁷⁸, P. Dervan⁷³, K. Desch²¹, E. Devetak¹⁴⁸, P.O. Deviveiros¹⁰⁵,
 A. Dewhurst¹²⁹, B. DeWilde¹⁴⁸, S. Dhaliwal¹⁵⁸, R. Dhullipudi^{25,n}, A. Di Ciaccio^{133a,133b},
 L. Di Ciaccio⁵, C. Di Donato^{102a,102b}, A. Di Girolamo³⁰, B. Di Girolamo³⁰, S. Di Luise^{134a,134b},
 A. Di Mattia¹⁵², B. Di Micco³⁰, R. Di Nardo⁴⁷, A. Di Simone^{133a,133b}, R. Di Sipio^{20a,20b},
 M.A. Diaz^{32a}, E.B. Diehl⁸⁷, J. Dietrich⁴², T.A. Dietzsch^{58a}, S. Diglio⁸⁶, K. Dindar Yagci⁴⁰,
 J. Dingfelder²¹, F. Dinut^{26a}, C. Dionisi^{132a,132b}, P. Dita^{26a}, S. Dita^{26a}, F. Dittus³⁰, F. Djama⁸³,
 T. Djobava^{51b}, M.A.B. do Vale^{24c}, A. Do Valle Wemans^{124a,o}, T.K.O. Doan⁵, M. Dobbs⁸⁵,
 D. Dobos³⁰, E. Dobson^{30,p}, J. Dodd³⁵, C. Doglioni⁴⁹, T. Doherty⁵³, Y. Doi^{65,*}, J. Dolejsi¹²⁷,
 Z. Dolezal¹²⁷, B.A. Dolgoshein^{96,*}, T. Dohmae¹⁵⁵, M. Donadelli^{24d}, J. Donini³⁴, J. Dopke³⁰,
 A. Doria^{102a}, A. Dos Anjos¹⁷³, A. Dotti^{122a,122b}, M.T. Dova⁷⁰, A.D. Doxiadis¹⁰⁵, A.T. Doyle⁵³,
 N. Dressnandt¹²⁰, M. Dris¹⁰, J. Dubbert⁹⁹, S. Dube¹⁵, E. Duchovni¹⁷², G. Duckeck⁹⁸, D. Duda¹⁷⁵,
 A. Dudarev³⁰, F. Dudziak⁶³, M. Dührssen³⁰, I.P. Duerdoth⁸², L. Duflot¹¹⁵, M-A. Dufour⁸⁵,
 L. Duguid⁷⁶, M. Dunford^{58a}, H. Duran Yildiz^{4a}, R. Duxfield¹³⁹, M. Dwuznik³⁸, M. Düren⁵²,
 W.L. Ebenstein⁴⁵, J. Ebke⁹⁸, S. Eckweiler⁸¹, K. Edmonds⁸¹, W. Edson², C.A. Edwards⁷⁶,
 N.C. Edwards⁵³, W. Ehrenfeld⁴², T. Eifert¹⁴³, G. Eigen¹⁴, K. Einsweiler¹⁵, E. Eisenhandler⁷⁵,
 T. Ekelof¹⁶⁶, M. El Kacimi^{135c}, M. Ellert¹⁶⁶, S. Elles⁵, F. Ellinghaus⁸¹, K. Ellis⁷⁵, N. Ellis³⁰,

J. Elmsheuser⁹⁸, M. Elsing³⁰, D. Emeliyanov¹²⁹, R. Engelmann¹⁴⁸, A. Engl⁹⁸, B. Epp⁶¹, J. Erdmann¹⁷⁶, A. Ereditato¹⁷, D. Eriksson^{146a}, J. Ernst², M. Ernst²⁵, J. Ernwein¹³⁶, D. Errede¹⁶⁵, S. Errede¹⁶⁵, E. Ertel⁸¹, M. Escalier¹¹⁵, H. Esch⁴³, C. Escobar¹²³, X. Espinal Curull¹², B. Esposito⁴⁷, F. Etienne⁸³, A.I. Etienvre¹³⁶, E. Etzion¹⁵³, D. Evangelakou⁵⁴, H. Evans⁶⁰, L. Fabbri^{20a,20b}, C. Fabre³⁰, R.M. Fakhruddinov¹²⁸, S. Falciano^{132a}, Y. Fang^{33a}, M. Fanti^{89a,89b}, A. Farbin⁸, A. Farilla^{134a}, J. Farley¹⁴⁸, T. Farooque¹⁵⁸, S. Farrell¹⁶³, S.M. Farrington¹⁷⁰, P. Farthouat³⁰, F. Fassi¹⁶⁷, P. Fassnacht³⁰, D. Fassouliotis⁹, B. Fatholahzadeh¹⁵⁸, A. Favareto^{89a,89b}, L. Fayard¹¹⁵, P. Federic^{144a}, O.L. Fedin¹²¹, W. Fedorko⁸⁸, M. Fehling-Kaschek⁴⁸, L. Felgioni⁸³, C. Feng^{33d}, E.J. Feng⁶, A.B. Fenyuk¹²⁸, J. Ferencei^{144b}, W. Fernando⁶, S. Ferrag⁵³, J. Ferrando⁵³, V. Ferrara⁴², A. Ferrari¹⁶⁶, P. Ferrari¹⁰⁵, R. Ferrari^{119a}, D.E. Ferreira de Lima⁵³, A. Ferrer¹⁶⁷, D. Ferrere⁴⁹, C. Ferretti⁸⁷, A. Ferretto Parodi^{50a,50b}, M. Fiascaris³¹, F. Fiedler⁸¹, A. Filipčić⁷⁴, F. Filthaut¹⁰⁴, M. Fincke-Keeler¹⁶⁹, M.C.N. Fiolhais^{124a,i}, L. Fiorini¹⁶⁷, A. Firan⁴⁰, G. Fischer⁴², M.J. Fisher¹⁰⁹, M. Flechl⁴⁸, I. Fleck¹⁴¹, J. Fleckner⁸¹, P. Fleischmann¹⁷⁴, S. Fleischmann¹⁷⁵, T. Flick¹⁷⁵, A. Floderus⁷⁹, L.R. Flores Castillo¹⁷³, A.C. Florez Bustos^{159b}, M.J. Flowerdew⁹⁹, T. Fonseca Martin¹⁷, A. Formica¹³⁶, A. Forti⁸², D. Fortin^{159a}, D. Fournier¹¹⁵, A.J. Fowler⁴⁵, H. Fox⁷¹, P. Francavilla¹², M. Franchini^{20a,20b}, S. Franchino^{119a,119b}, D. Francis³⁰, T. Frank¹⁷², M. Franklin⁵⁷, S. Franz³⁰, M. Fraternali^{119a,119b}, S. Fratina¹²⁰, S.T. French²⁸, C. Friedrich⁴², F. Friedrich⁴⁴, D. Froidevaux³⁰, J.A. Frost²⁸, C. Fukunaga¹⁵⁶, E. Fullana Torregrosa¹²⁷, B.G. Fulsom¹⁴³, J. Fuster¹⁶⁷, C. Gabaldon³⁰, O. Gabizon¹⁷², T. Gadfort²⁵, S. Gadomski⁴⁹, G. Gagliardi^{50a,50b}, P. Gagnon⁶⁰, C. Galea⁹⁸, B. Galhardo^{124a}, E.J. Gallas¹¹⁸, V. Gallo¹⁷, B.J. Gallop¹²⁹, P. Gallus¹²⁵, K.K. Gan¹⁰⁹, Y.S. Gao^{143,g}, A. Gaponenko¹⁵, F. Garbersen¹⁷⁶, M. Garcia-Sciveres¹⁵, C. García¹⁶⁷, J.E. García Navarro¹⁶⁷, R.W. Gardner³¹, N. Garelli³⁰, V. Garonne³⁰, C. Gatti⁴⁷, G. Gaudio^{119a}, B. Gaur¹⁴¹, L. Gauthier¹³⁶, P. Gauzzi^{132a,132b}, I.L. Gavrilenko⁹⁴, C. Gay¹⁶⁸, G. Gaycken²¹, E.N. Gazis¹⁰, P. Ge^{33d}, Z. Gecse¹⁶⁸, C.N.P. Gee¹²⁹, D.A.A. Geerts¹⁰⁵, Ch. Geich-Gimbel²¹, K. Gellerstedt^{146a,146b}, C. Gemme^{50a}, A. Gemmel⁵³, M.H. Genest⁵⁵, S. Gentile^{132a,132b}, M. George⁵⁴, S. George⁷⁶, D. Gerbaudo¹², P. Gerlach¹⁷⁵, A. Gershon¹⁵³, C. Geweniger^{58a}, H. Ghazlane^{135b}, N. Ghodbane³⁴, B. Giacobbe^{20a}, S. Giagu^{132a,132b}, V. Giangiobbe¹², F. Gianotti³⁰, B. Gibbard²⁵, A. Gibson¹⁵⁸, S.M. Gibson³⁰, M. Gilchriese¹⁵, D. Gillberg²⁹, A.R. Gillman¹²⁹, D.M. Gingrich^{3,f}, J. Ginzburg¹⁵³, N. Giokaris⁹, M.P. Giordani^{164c}, R. Giordano^{102a,102b}, F.M. Giorgi¹⁶, P. Giovannini⁹⁹, P.F. Giraud¹³⁶, D. Giugni^{89a}, M. Giunta⁹³, B.K. Gjelsten¹¹⁷, L.K. Gladilin⁹⁷, C. Glasman⁸⁰, J. Glatzer²¹, A. Glazov⁴², K.W. Glitza¹⁷⁵, G.L. Glonti⁶⁴, J.R. Goddard⁷⁵, J. Godfrey¹⁴², J. Godlewski³⁰, M. Goebel⁴², T. Göpfert⁴⁴, C. Goeringer⁸¹, C. Gössling⁴³, S. Goldfarb⁸⁷, T. Golling¹⁷⁶, D. Golubkov¹²⁸, A. Gomes^{124a,c}, L.S. Gomez Fajardo⁴², R. Gonçalves⁷⁶, J. Goncalves Pinto Firmino Da Costa⁴², L. Gonella²¹, S. González de la Hoz¹⁶⁷, G. Gonzalez Parra¹², M.L. Gonzalez Silva²⁷, S. Gonzalez-Sevilla⁴⁹, J.J. Goodson¹⁴⁸, L. Goossens³⁰, P.A. Gorbounov⁹⁵, H.A. Gordon²⁵, I. Gorelov¹⁰³, G. Gorfine¹⁷⁵, B. Gorini³⁰, E. Gorini^{72a,72b}, A. Gorišek⁷⁴, E. Gornicki³⁹, A.T. Goshaw⁶, M. Gosselink¹⁰⁵, M.I. Gostkin⁶⁴, I. Gough Eschrich¹⁶³, M. Gouighri^{135a}, D. Goujdami^{135c}, M.P. Goulette⁴⁹, A.G. Goussiou¹³⁸, C. Goy⁵, S. Gozpinar²³, I. Grabowska-Bold³⁸, P. Grafström^{20a,20b}, K.-J. Grahn⁴², E. Gramstad¹¹⁷, F. Grancagnolo^{72a}, S. Grancagnolo¹⁶, V. Grassi¹⁴⁸, V. Gratchev¹²¹, N. Grau³⁵, H.M. Gray³⁰, J.A. Gray¹⁴⁸, E. Graziani^{134a}, O.G. Grebenyuk¹²¹, T. Greenshaw⁷³, Z.D. Greenwood^{25,n}, K. Gregersen³⁶, I.M. Gregor⁴², P. Grenier¹⁴³, J. Griffiths⁸,

N. Grigalashvili⁶⁴, A.A. Grillo¹³⁷, S. Grinstein¹², Ph. Gris³⁴, Y.V. Grishkevich⁹⁷, J.-F. Grivaz¹¹⁵,
 A. Grohsjean⁴², E. Gross¹⁷², J. Grosse-Knetter⁵⁴, J. Groth-Jensen¹⁷², K. Grybel¹⁴¹, D. Guest¹⁷⁶,
 C. Guicheney³⁴, E. Guido^{50a,50b}, S. Guindon⁵⁴, U. Gul⁵³, J. Gunther¹²⁵, B. Guo¹⁵⁸, J. Guo³⁵,
 P. Gutierrez¹¹¹, N. Guttman¹⁵³, O. Gutzwiller¹⁷³, C. Guyot¹³⁶, C. Gwenlan¹¹⁸, C.B. Gwilliam⁷³,
 A. Haas¹⁰⁸, S. Haas³⁰, C. Haber¹⁵, H.K. Hadavand⁸, D.R. Hadley¹⁸, P. Haefner²¹, F. Hahn³⁰,
 Z. Hajduk³⁹, H. Hakobyan¹⁷⁷, D. Hall¹¹⁸, K. Hamacher¹⁷⁵, P. Hamal¹¹³, K. Hamano⁸⁶,
 M. Hamer⁵⁴, A. Hamilton^{145b,q}, S. Hamilton¹⁶¹, L. Han^{33b}, K. Hanagaki¹¹⁶, K. Hanawa¹⁶⁰,
 M. Hance¹⁵, C. Handel⁸¹, P. Hanke^{58a}, J.R. Hansen³⁶, J.B. Hansen³⁶, J.D. Hansen³⁶,
 P.H. Hansen³⁶, P. Hansson¹⁴³, K. Hara¹⁶⁰, T. Harenberg¹⁷⁵, S. Harkusha⁹⁰, D. Harper⁸⁷,
 R.D. Harrington⁴⁶, O.M. Harris¹³⁸, J. Hartert⁴⁸, F. Hartjes¹⁰⁵, T. Haruyama⁶⁵, A. Harvey⁵⁶,
 S. Hasegawa¹⁰¹, Y. Hasegawa¹⁴⁰, S. Hassani¹³⁶, S. Haug¹⁷, M. Hauschild³⁰, R. Hauser⁸⁸,
 M. Havranek²¹, C.M. Hawkes¹⁸, R.J. Hawkins³⁰, A.D. Hawkins⁷⁹, T. Hayakawa⁶⁶,
 T. Hayashi¹⁶⁰, D. Hayden⁷⁶, C.P. Hays¹¹⁸, H.S. Hayward⁷³, S.J. Haywood¹²⁹, S.J. Head¹⁸,
 V. Hedberg⁷⁹, L. Heelan⁸, S. Heim¹²⁰, B. Heinemann¹⁵, S. Heisterkamp³⁶, L. Helary²²,
 C. Heller⁹⁸, M. Heller³⁰, S. Hellman^{146a,146b}, D. Hellmich²¹, C. Helsens¹², R.C.W. Henderson⁷¹,
 M. Henke^{58a}, A. Henrichs¹⁷⁶, A.M. Henriques Correia³⁰, S. Henrot-Versille¹¹⁵, C. Hensel⁵⁴,
 C.M. Hernandez⁸, Y. Hernández Jiménez¹⁶⁷, R. Herrberg¹⁶, G. Herten⁴⁸, R. Hertenberger⁹⁸,
 L. Hervas³⁰, G.G. Hesketh⁷⁷, N.P. Hessey¹⁰⁵, E. Higón-Rodríguez¹⁶⁷, J.C. Hill²⁸, K.H. Hiller⁴²,
 S. Hillert²¹, S.J. Hillier¹⁸, I. Hinchliffe¹⁵, E. Hines¹²⁰, M. Hirose¹¹⁶, F. Hirsch⁴³,
 D. Hirschbuehl¹⁷⁵, J. Hobbs¹⁴⁸, N. Hod¹⁵³, M.C. Hodgkinson¹³⁹, P. Hodgson¹³⁹, A. Hoecker³⁰,
 M.R. Hoferkamp¹⁰³, J. Hoffman⁴⁰, D. Hoffmann⁸³, M. Hohlfield⁸¹, M. Holder¹⁴¹,
 S.O. Holmgren^{146a}, T. Holy¹²⁶, J.L. Holzbauer⁸⁸, T.M. Hong¹²⁰, L. Hooft van Huysduynen¹⁰⁸,
 S. Horner⁴⁸, J-Y. Hostachy⁵⁵, S. Hou¹⁵¹, A. Houmada^{135a}, J. Howard¹¹⁸, J. Howarth⁸²,
 I. Hristova¹⁶, J. Hrivnac¹¹⁵, T. Hryn'ova⁵, P.J. Hsu⁸¹, S.-C. Hsu¹³⁸, D. Hu³⁵, Z. Hubacek³⁰,
 F. Hubaut⁸³, F. Huegging²¹, A. Huettmann⁴², T.B. Huffman¹¹⁸, E.W. Hughes³⁵, G. Hughes⁷¹,
 M. Huhtinen³⁰, M. Hurwitz¹⁵, N. Huseynov^{64,r}, J. Huston⁸⁸, J. Huth⁵⁷, G. Iacobucci⁴⁹,
 G. Iakovidis¹⁰, M. Ibbotson⁸², I. Ibragimov¹⁴¹, L. Iconomidou-Fayard¹¹⁵, J. Idarraga¹¹⁵,
 P. Iengo^{102a}, O. Igonkina¹⁰⁵, Y. Ikegami⁶⁵, M. Ikeno⁶⁵, D. Iliadis¹⁵⁴, N. Ilic¹⁵⁸, T. Ince⁹⁹,
 P. Ioannou⁹, M. Iodice^{134a}, K. Iordanidou⁹, V. Ippolito^{132a,132b}, A. Irls Quiles¹⁶⁷, C. Isaksson¹⁶⁶,
 M. Ishino⁶⁷, M. Ishitsuka¹⁵⁷, R. Ishmukhametov¹⁰⁹, C. Issever¹¹⁸, S. Istin^{19a}, A.V. Ivashin¹²⁸,
 W. Iwanski³⁹, H. Iwasaki⁶⁵, J.M. Izen⁴¹, V. Izzo^{102a}, B. Jackson¹²⁰, J.N. Jackson⁷³, P. Jackson¹,
 M.R. Jaekel³⁰, V. Jain², K. Jakobs⁴⁸, S. Jakobsen³⁶, T. Jakoubek¹²⁵, J. Jakubek¹²⁶, D.O. Jamin¹⁵¹,
 D.K. Jana¹¹¹, E. Jansen⁷⁷, H. Jansen³⁰, J. Janssen²¹, A. Jantsch⁹⁹, M. Janus⁴⁸, R.C. Jared¹⁷³,
 G. Jarlskog⁷⁹, L. Jeanty⁵⁷, I. Jen-La Plante³¹, G.-Y. Jeng¹⁵⁰, D. Jennens⁸⁶, P. Jenni³⁰,
 A.E. Loevschall-Jensen³⁶, P. Jež³⁶, S. Jézéquel⁵, M.K. Jha^{20a}, H. Ji¹⁷³, W. Ji⁸¹, J. Jia¹⁴⁸,
 Y. Jiang^{33b}, M. Jimenez Belenguer⁴², S. Jin^{33a}, O. Jinnouchi¹⁵⁷, M.D. Joergensen³⁶, D. Joffe⁴⁰,
 M. Johansen^{146a,146b}, K.E. Johansson^{146a}, P. Johansson¹³⁹, S. Johnert⁴², K.A. Johns⁷,
 K. Jon-And^{146a,146b}, G. Jones¹⁷⁰, R.W.L. Jones⁷¹, T.J. Jones⁷³, C. Joram³⁰, P.M. Jorge^{124a},
 K.D. Joshi⁸², J. Jovicevic¹⁴⁷, T. Jovin^{13b}, X. Ju¹⁷³, C.A. Jung⁴³, R.M. Jungst³⁰, V. Juranek¹²⁵,
 P. Jussel⁶¹, A. Juste Rozas¹², S. Kabana¹⁷, M. Kaci¹⁶⁷, A. Kaczmarzka³⁹, P. Kadlecik³⁶,
 M. Kado¹¹⁵, H. Kagan¹⁰⁹, M. Kagan⁵⁷, E. Kajomovitz¹⁵², S. Kalinin¹⁷⁵, L.V. Kalinovskaya⁶⁴,
 S. Kama⁴⁰, N. Kanaya¹⁵⁵, M. Kaneda³⁰, S. Kaneti²⁸, T. Kanno¹⁵⁷, V.A. Kantserov⁹⁶, J. Kanzaki⁶⁵,
 B. Kaplan¹⁰⁸, A. Kapliy³¹, D. Kar⁵³, M. Karagounis²¹, K. Karakostas¹⁰, M. Karnevskiy^{58b},

V. Kartvelishvili⁷¹, A.N. Karyukhin¹²⁸, L. Kashif¹⁷³, G. Kasieczka^{58b}, R.D. Kass¹⁰⁹,
A. Kastanas¹⁴, M. Kataoka⁵, Y. Kataoka¹⁵⁵, J. Katzy⁴², V. Kaushik⁷, K. Kawagoe⁶⁹,
T. Kawamoto¹⁵⁵, G. Kawamura⁸¹, M.S. Kayl¹⁰⁵, S. Kazama¹⁵⁵, V.F. Kazanin¹⁰⁷,
M.Y. Kazarinov⁶⁴, R. Keeler¹⁶⁹, P.T. Keener¹²⁰, R. Kehoe⁴⁰, M. Keil⁵⁴, G.D. Kekelidze⁶⁴,
J.S. Keller¹³⁸, M. Kenyon⁵³, O. Kepka¹²⁵, N. Kerschen³⁰, B.P. Kerševan⁷⁴, S. Kersten¹⁷⁵,
K. Kessoku¹⁵⁵, J. Keung¹⁵⁸, F. Khalil-zada¹¹, H. Khandanyan^{146a,146b}, A. Khanov¹¹²,
D. Kharchenko⁶⁴, A. Khodinov⁹⁶, A. Khomich^{58a}, T.J. Khoo²⁸, G. Khoriauli²¹,
A. Khoroshilov¹⁷⁵, V. Khovanskiy⁹⁵, E. Khramov⁶⁴, J. Khubua^{51b}, H. Kim^{146a,146b}, S.H. Kim¹⁶⁰,
N. Kimura¹⁷¹, O. Kind¹⁶, B.T. King⁷³, M. King⁶⁶, R.S.B. King¹¹⁸, J. Kirk¹²⁹, A.E. Kiryunin⁹⁹,
T. Kishimoto⁶⁶, D. Kisielewska³⁸, T. Kitamura⁶⁶, T. Kittelmann¹²³, K. Kiuchi¹⁶⁰, E. Kladiva^{144b},
M. Klein⁷³, U. Klein⁷³, K. Kleinknecht⁸¹, M. Klemetti⁸⁵, A. Klier¹⁷², P. Klimek^{146a,146b},
A. Klimentov²⁵, R. Klingenberg⁴³, J.A. Klinger⁸², E.B. Klinkby³⁶, T. Klioutchnikova³⁰,
P.F. Klok¹⁰⁴, S. Klous¹⁰⁵, E.-E. Kluge^{58a}, T. Kluge⁷³, P. Kluit¹⁰⁵, S. Kluth⁹⁹, E. Kneringer⁶¹,
E.B.F.G. Knoops⁸³, A. Knue⁵⁴, B.R. Ko⁴⁵, T. Kobayashi¹⁵⁵, M. Kobel⁴⁴, M. Kocian¹⁴³,
P. Kodys¹²⁷, K. Köneke³⁰, A.C. König¹⁰⁴, S. Koenig⁸¹, L. Köpke⁸¹, F. Koetsveld¹⁰⁴,
P. Koevesarki²¹, T. Koffas²⁹, E. Koffeman¹⁰⁵, L.A. Kogan¹¹⁸, S. Kohlmann¹⁷⁵, F. Kohn⁵⁴,
Z. Kohout¹²⁶, T. Kohriki⁶⁵, T. Koi¹⁴³, G.M. Kolachev^{107,*}, H. Kolanoski¹⁶, V. Kolesnikov⁶⁴,
I. Koletsou^{89a}, J. Koll⁸⁸, A.A. Komar⁹⁴, Y. Komori¹⁵⁵, T. Kondo⁶⁵, T. Kono^{42,s}, A.I. Kononov⁴⁸,
R. Konoplich^{108,t}, N. Konstantinidis⁷⁷, R. Kopeliansky¹⁵², S. Koperny³⁸, K. Korcyl³⁹,
K. Kordas¹⁵⁴, A. Korn¹¹⁸, A. Korol¹⁰⁷, I. Korolkov¹², E.V. Korolkova¹³⁹, V.A. Korotkov¹²⁸,
O. Kortner⁹⁹, S. Kortner⁹⁹, V.V. Kostyukhin²¹, S. Kotov⁹⁹, V.M. Kotov⁶⁴, A. Kotwal⁴⁵,
C. Kourkoumelis⁹, V. Kouskoura¹⁵⁴, A. Koutsman^{159a}, R. Kowalewski¹⁶⁹, T.Z. Kowalski³⁸,
W. Kozanecki¹³⁶, A.S. Kozhin¹²⁸, V. Kral¹²⁶, V.A. Kramarenko⁹⁷, G. Kramberger⁷⁴,
M.W. Krasny⁷⁸, A. Krasznahorkay¹⁰⁸, J.K. Kraus²¹, A. Kravchenko²⁵, S. Kreiss¹⁰⁸, F. Krejci¹²⁶,
J. Kretschmar⁷³, K. Kreutzfeldt⁵², N. Krieger⁵⁴, P. Krieger¹⁵⁸, K. Kroeninger⁵⁴, H. Kroha⁹⁹,
J. Kroll¹²⁰, J. Kroseberg²¹, J. Krstic^{13a}, U. Kruchonak⁶⁴, H. Krüger²¹, T. Kruker¹⁷,
N. Krumnack⁶³, Z.V. Krumshteyn⁶⁴, M.K. Kruse⁴⁵, T. Kubota⁸⁶, S. Kудay^{4a}, S. Kuehn⁴⁸,
A. Kugel^{58c}, T. Kuhl⁴², D. Kuhn⁶¹, V. Kukhtin⁶⁴, Y. Kulchitsky⁹⁰, S. Kuleshov^{32b}, C. Kummer⁹⁸,
M. Kuna⁷⁸, J. Kunkle¹²⁰, A. Kupco¹²⁵, H. Kurashige⁶⁶, M. Kurata¹⁶⁰, Y.A. Kurochkin⁹⁰,
V. Kus¹²⁵, E.S. Kuwertz¹⁴⁷, M. Kuze¹⁵⁷, J. Kvita¹⁴², R. Kwee¹⁶, A. La Rosa⁴⁹,
L. La Rotonda^{37a,37b}, L. Labarga⁸⁰, S. Lablak^{135a}, C. Lacasta¹⁶⁷, F. Lacava^{132a,132b}, J. Lacey²⁹,
H. Lacker¹⁶, D. Lacour⁷⁸, V.R. Lacuesta¹⁶⁷, E. Ladygin⁶⁴, R. Lafaye⁵, B. Laforge⁷⁸,
T. Lagouri¹⁷⁶, S. Lai⁴⁸, E. Laisne⁵⁵, L. Lambourne⁷⁷, C.L. Lampen⁷, W. Lampl⁷, E. Lancon¹³⁶,
U. Landgraf⁴⁸, M.P.J. Landon⁷⁵, V.S. Lang^{58a}, C. Lange⁴², A.J. Lankford¹⁶³, F. Lanni²⁵,
K. Lantzsch³⁰, A. Lanza^{119a}, S. Laplace⁷⁸, C. Lapoire²¹, J.F. Laporte¹³⁶, T. Lari^{89a}, A. Larner¹¹⁸,
M. Lassnig³⁰, P. Laurelli⁴⁷, V. Lavorini^{37a,37b}, W. Lavrijsen¹⁵, P. Laycock⁷³, O. Le Dortz⁷⁸,
E. Le Guirriec⁸³, E. Le Menedeu¹², T. LeCompte⁶, F. Ledroit-Guillon⁵⁵, H. Lee¹⁰⁵, J.S.H. Lee¹¹⁶,
S.C. Lee¹⁵¹, L. Lee¹⁷⁶, M. Lefebvre¹⁶⁹, M. Legendre¹³⁶, F. Legger⁹⁸, C. Leggett¹⁵,
M. Lehmacher²¹, G. Lehmann Miotto³⁰, A.G. Leister¹⁷⁶, M.A.L. Leite^{24d}, R. Leitner¹²⁷,
D. Lellouch¹⁷², B. Lemmer⁵⁴, V. Lendermann^{58a}, K.J.C. Leney^{145b}, T. Lenz¹⁰⁵, G. Lenzen¹⁷⁵,
B. Lenzi³⁰, K. Leonhardt⁴⁴, S. Leontsinis¹⁰, F. Lepold^{58a}, C. Leroy⁹³, J-R. Lessard¹⁶⁹,
C.G. Lester²⁸, C.M. Lester¹²⁰, J. Levêque⁵, D. Levin⁸⁷, L.J. Levinson¹⁷², A. Lewis¹¹⁸,
G.H. Lewis¹⁰⁸, A.M. Leyko²¹, M. Leyton¹⁶, B. Li^{33b}, B. Li⁸³, H. Li¹⁴⁸, H.L. Li³¹, S. Li^{33b,u},

X. Li⁸⁷, Z. Liang^{118,v}, H. Liao³⁴, B. Liberti^{133a}, P. Lichard³⁰, M. Lichtnecker⁹⁸, K. Lie¹⁶⁵, W. Liebig¹⁴, C. Limbach²¹, A. Limosani⁸⁶, M. Limper⁶², S.C. Lin^{151,w}, F. Linde¹⁰⁵, J.T. Linnemann⁸⁸, E. Lipeles¹²⁰, A. Lipniacka¹⁴, T.M. Liss¹⁶⁵, D. Lissauer²⁵, A. Lister⁴⁹, A.M. Litke¹³⁷, C. Liu²⁹, D. Liu¹⁵¹, J.B. Liu⁸⁷, L. Liu⁸⁷, M. Liu^{33b}, Y. Liu^{33b}, M. Livan^{119a,119b}, S.S.A. Livermore¹¹⁸, A. Lleres⁵⁵, J. Llorente Merino⁸⁰, S.L. Lloyd⁷⁵, E. Lobodzinska⁴², P. Loch⁷, W.S. Lockman¹³⁷, T. Loddenkoetter²¹, F.K. Loebinger⁸², A. Loginov¹⁷⁶, C.W. Loh¹⁶⁸, T. Lohse¹⁶, K. Lohwasser⁴⁸, M. Lokajicek¹²⁵, V.P. Lombardo⁵, R.E. Long⁷¹, L. Lopes^{124a}, D. Lopez Mateos⁵⁷, J. Lorenz⁹⁸, N. Lorenzo Martinez¹¹⁵, M. Losada¹⁶², P. Loscutoff¹⁵, F. Lo Sterzo^{132a,132b}, M.J. Losty^{159a,*}, X. Lou⁴¹, A. Lounis¹¹⁵, K.F. Loureiro¹⁶², J. Love⁶, P.A. Love⁷¹, A.J. Lowe^{143,g}, F. Lu^{33a}, H.J. Lubatti¹³⁸, C. Luci^{132a,132b}, A. Lucotte⁵⁵, D. Ludwig⁴², I. Ludwig⁴⁸, J. Ludwig⁴⁸, F. Luehring⁶⁰, G. Luijckx¹⁰⁵, W. Lukas⁶¹, L. Luminari^{132a}, E. Lund¹¹⁷, B. Lund-Jensen¹⁴⁷, B. Lundberg⁷⁹, J. Lundberg^{146a,146b}, O. Lundberg^{146a,146b}, J. Lundquist³⁶, M. Lungwitz⁸¹, D. Lynn²⁵, E. Lytken⁷⁹, H. Ma²⁵, L.L. Ma¹⁷³, G. Maccarrone⁴⁷, A. Macchiolo⁹⁹, B. Maček⁷⁴, J. Machado Miguens^{124a}, D. Macina³⁰, R. Mackeprang³⁶, R.J. Madaras¹⁵, H.J. Maddocks⁷¹, W.F. Mader⁴⁴, R. Maenner^{58c}, T. Maeno²⁵, P. Mättig¹⁷⁵, S. Mättig⁴², L. Magnoni¹⁶³, E. Magradze⁵⁴, K. Mahboubi⁴⁸, J. Mahlstedt¹⁰⁵, S. Mahmoud⁷³, G. Mahout¹⁸, C. Maiani¹³⁶, C. Maidantchik^{24a}, A. Maio^{124a,c}, S. Majewski²⁵, Y. Makida⁶⁵, N. Makovec¹¹⁵, P. Mal¹³⁶, B. Malaescu³⁰, Pa. Malecki³⁹, P. Malecki³⁹, V.P. Maleev¹²¹, F. Malek⁵⁵, U. Mallik⁶², D. Malon⁶, C. Malone¹⁴³, S. Maltezos¹⁰, V. Malyshev¹⁰⁷, S. Malyukov³⁰, J. Mamuzic^{13b}, A. Manabe⁶⁵, L. Mandelli^{89a}, I. Mandić⁷⁴, R. Mandrysch⁶², J. Maneira^{124a}, A. Manfredini⁹⁹, L. Manhaes de Andrade Filho^{24b}, J.A. Manjarres Ramos¹³⁶, A. Mann⁹⁸, P.M. Manning¹³⁷, A. Manousakis-Katsikakis⁹, B. Mansoulie¹³⁶, R. Mantifel⁸⁵, A. Mapelli³⁰, L. Mapelli³⁰, L. March¹⁶⁷, J.F. Marchand²⁹, F. Marchese^{133a,133b}, G. Marchiori⁷⁸, M. Marcisovsky¹²⁵, C.P. Marino¹⁶⁹, F. Marroquim^{24a}, Z. Marshall³⁰, L.F. Marti¹⁷, S. Marti-Garcia¹⁶⁷, B. Martin³⁰, B. Martin⁸⁸, J.P. Martin⁹³, T.A. Martin¹⁸, V.J. Martin⁴⁶, B. Martin dit Latour⁴⁹, S. Martin-Haugh¹⁴⁹, H. Martinez¹³⁶, M. Martinez¹², V. Martinez Outschoorn⁵⁷, A.C. Martyniuk¹⁶⁹, M. Marx⁸², F. Marzano^{132a}, A. Marzin¹¹¹, L. Masetti⁸¹, T. Mashimo¹⁵⁵, R. Mashinistov⁹⁴, J. Masik⁸², A.L. Maslennikov¹⁰⁷, I. Massa^{20a,20b}, G. Massaro¹⁰⁵, N. Massol⁵, P. Mastrandrea¹⁴⁸, A. Mastroberardino^{37a,37b}, T. Masubuchi¹⁵⁵, H. Matsunaga¹⁵⁵, T. Matsushita⁶⁶, C. Mattraversi^{118,d}, J. Maurer⁸³, S.J. Maxfield⁷³, D.A. Maximov^{107,h}, A. Mayne¹³⁹, R. Mazini¹⁵¹, M. Mazur²¹, L. Mazzaferro^{133a,133b}, M. Mazzanti^{89a}, J. Mc Donald⁸⁵, S.P. Mc Kee⁸⁷, A. McCarn¹⁶⁵, R.L. McCarthy¹⁴⁸, T.G. McCarthy²⁹, N.A. McCubbin¹²⁹, K.W. McFarlane^{56,*}, J.A. Mcfayden¹³⁹, G. Mchedlidze^{51b}, T. Mclaughlan¹⁸, S.J. McMahon¹²⁹, R.A. McPherson^{169,i}, A. Meade⁸⁴, J. Mechnich¹⁰⁵, M. Mechtel¹⁷⁵, M. Medinnis⁴², S. Meehan³¹, R. Meera-Lebbai¹¹¹, T. Meguro¹¹⁶, S. Mehlhase³⁶, A. Mehta⁷³, K. Meier^{58a}, B. Meirose⁷⁹, C. Melachrinou³¹, B.R. Mellado Garcia¹⁷³, F. Meloni^{89a,89b}, L. Mendoza Navas¹⁶², Z. Meng^{151,x}, A. Mengarelli^{20a,20b}, S. Menke⁹⁹, E. Meoni¹⁶¹, K.M. Mercurio⁵⁷, P. Mermod⁴⁹, L. Merola^{102a,102b}, C. Meroni^{89a}, F.S. Merritt³¹, H. Merritt¹⁰⁹, A. Messina^{30,y}, J. Metcalfe²⁵, A.S. Mete¹⁶³, C. Meyer⁸¹, C. Meyer³¹, J-P. Meyer¹³⁶, J. Meyer¹⁷⁴, J. Meyer⁵⁴, S. Michal³⁰, L. Micu^{26a}, R.P. Middleton¹²⁹, S. Migas⁷³, L. Mijović¹³⁶, G. Mikenberg¹⁷², M. Míkštíkova¹²⁵, M. Mikuž⁷⁴, D.W. Miller³¹, R.J. Miller⁸⁸, W.J. Mills¹⁶⁸, C. Mills⁵⁷, A. Milov¹⁷², D.A. Milstead^{146a,146b}, D. Milstein¹⁷², A.A. Minaenko¹²⁸, M. Miñano Moya¹⁶⁷, I.A. Minashvili⁶⁴, A.I. Mincer¹⁰⁸, B. Mindur³⁸, M. Mineev⁶⁴, Y. Ming¹⁷³, L.M. Mir¹², G. Mirabelli^{132a}, J. Mitrevski¹³⁷,

V.A. Mitsou¹⁶⁷, S. Mitsui⁶⁵, P.S. Miyagawa¹³⁹, J.U. Mjörnmark⁷⁹, T. Moa^{146a,146b}, V. Moeller²⁸, K. Mönig⁴², N. Möser²¹, S. Mohapatra¹⁴⁸, W. Mohr⁴⁸, R. Moles-Valls¹⁶⁷, A. Molfetas³⁰, J. Monk⁷⁷, E. Monnier⁸³, J. Montejó Berlingen¹², F. Monticelli⁷⁰, S. Monzani^{20a,20b}, R.W. Moore³, G.F. Moorhead⁸⁶, C. Mora Herrera⁴⁹, A. Moraes⁵³, N. Morange¹³⁶, J. Morel⁵⁴, G. Morello^{37a,37b}, D. Moreno⁸¹, M. Moreno Llácer¹⁶⁷, P. Morettini^{50a}, M. Morgenstern⁴⁴, M. Morii⁵⁷, A.K. Morley³⁰, G. Mornacchi³⁰, J.D. Morris⁷⁵, L. Morvaj¹⁰¹, H.G. Moser⁹⁹, M. Mosidze^{51b}, J. Moss¹⁰⁹, R. Mount¹⁴³, E. Mountricha^{10,z}, S.V. Mouraviev^{94,*}, E.J.W. Moyses⁸⁴, F. Mueller^{58a}, J. Mueller¹²³, K. Mueller²¹, T.A. Müller⁹⁸, T. Mueller⁸¹, D. Muenstermann³⁰, Y. Munwes¹⁵³, W.J. Murray¹²⁹, I. Mussche¹⁰⁵, E. Musto¹⁵², A.G. Myagkov¹²⁸, M. Myska¹²⁵, O. Nackenhorst⁵⁴, J. Nadal¹², K. Nagai¹⁶⁰, R. Nagai¹⁵⁷, K. Nagano⁶⁵, A. Nagarkar¹⁰⁹, Y. Nagasaka⁵⁹, M. Nagel⁹⁹, A.M. Nairz³⁰, Y. Nakahama³⁰, K. Nakamura¹⁵⁵, T. Nakamura¹⁵⁵, I. Nakano¹¹⁰, G. Nanava²¹, A. Napier¹⁶¹, R. Narayan^{58b}, M. Nash^{77,d}, T. Nattermann²¹, T. Naumann⁴², G. Navarro¹⁶², H.A. Neal⁸⁷, P.Yu. Nechaeva⁹⁴, T.J. Neep⁸², A. Negri^{119a,119b}, G. Negri³⁰, M. Negrini^{20a}, S. Nektarijevic⁴⁹, A. Nelson¹⁶³, T.K. Nelson¹⁴³, S. Nemecek¹²⁵, P. Nemethy¹⁰⁸, A.A. Nepomuceno^{24a}, M. Nessi^{30,aa}, M.S. Neubauer¹⁶⁵, M. Neumann¹⁷⁵, A. Neusiedl⁸¹, R.M. Neves¹⁰⁸, P. Nevski²⁵, F.M. Newcomer¹²⁰, P.R. Newman¹⁸, V. Nguyen Thi Hong¹³⁶, R.B. Nickerson¹¹⁸, R. Nicolaidou¹³⁶, B. Nicquevert³⁰, F. Niedercorn¹¹⁵, J. Nielsen¹³⁷, N. Nikiforou³⁵, A. Nikiforov¹⁶, V. Nikolaenko¹²⁸, I. Nikolic-Audit⁷⁸, K. Nikolics⁴⁹, K. Nikolopoulos¹⁸, H. Nilsen⁴⁸, P. Nilsson⁸, Y. Ninomiya¹⁵⁵, A. Nisati^{132a}, R. Nisius⁹⁹, T. Nobe¹⁵⁷, L. Nodulman⁶, M. Nomachi¹¹⁶, I. Nomidis¹⁵⁴, S. Norberg¹¹¹, M. Nordberg³⁰, J. Novakova¹²⁷, M. Nozaki⁶⁵, L. Nozka¹¹³, I.M. Nugent^{159a}, A.-E. Nuncio-Quiroz²¹, G. Nunes Hanninger⁸⁶, T. Nunnemann⁹⁸, E. Nurse⁷⁷, B.J. O'Brien⁴⁶, D.C. O'Neil¹⁴², V. O'Shea⁵³, L.B. Oakes⁹⁸, F.G. Oakham^{29,f}, H. Oberlack⁹⁹, J. Ocariz⁷⁸, A. Ochi⁶⁶, S. Oda⁶⁹, S. Odaka⁶⁵, J. Odier⁸³, H. Ogren⁶⁰, A. Oh⁸², S.H. Oh⁴⁵, C.C. Ohm³⁰, T. Ohshima¹⁰¹, W. Okamura¹¹⁶, H. Okawa²⁵, Y. Okumura³¹, T. Okuyama¹⁵⁵, A. Olariu^{26a}, A.G. Olchevski⁶⁴, S.A. Olivares Pino^{32a}, M. Oliveira^{124a,i}, D. Oliveira Damazio²⁵, E. Oliver Garcia¹⁶⁷, D. Olivito¹²⁰, A. Olszewski³⁹, J. Olszowska³⁹, A. Onofre^{124a,ab}, P.U.E. Onyisi^{31,ac}, C.J. Oram^{159a}, M.J. Oreglia³¹, Y. Oren¹⁵³, D. Orestano^{134a,134b}, N. Orlando^{72a,72b}, I. Orlov¹⁰⁷, C. Oropeza Barrera⁵³, R.S. Orr¹⁵⁸, B. Osculati^{50a,50b}, R. Ospanov¹²⁰, C. Osuna¹², G. Otero y Garzon²⁷, J.P. Ottersbach¹⁰⁵, M. Ouchrif^{135d}, E.A. Ouellette¹⁶⁹, F. Ould-Saada¹¹⁷, A. Ouraou¹³⁶, Q. Ouyang^{33a}, A. Ovcharova¹⁵, M. Owen⁸², S. Owen¹³⁹, V.E. Ozcan^{19a}, N. Ozturk⁸, A. Pacheco Pages¹², C. Padilla Aranda¹², S. Pagan Griso¹⁵, E. Paganis¹³⁹, C. Pahl⁹⁹, F. Paige²⁵, P. Pais⁸⁴, K. Pajchel¹¹⁷, G. Palacino^{159b}, C.P. Paleari⁷, S. Palestini³⁰, D. Pallin³⁴, A. Palma^{124a}, J.D. Palmer¹⁸, Y.B. Pan¹⁷³, E. Panagiotopoulou¹⁰, J.G. Panduro Vazquez⁷⁶, P. Pani¹⁰⁵, N. Panikashvili⁸⁷, S. Panitkin²⁵, D. Pantea^{26a}, A. Papadelis^{146a}, Th.D. Papadopoulos¹⁰, A. Paramonov⁶, D. Paredes Hernandez³⁴, W. Park^{25,ad}, M.A. Parker²⁸, F. Parodi^{50a,50b}, J.A. Parsons³⁵, U. Parzefall⁴⁸, S. Pashapour⁵⁴, E. Pasqualucci^{132a}, S. Passaggio^{50a}, A. Passeri^{134a}, F. Pastore^{134a,134b,*}, Fr. Pastore⁷⁶, G. Pásztor^{49,ae}, S. Pataria¹⁷⁵, N. Patel¹⁵⁰, J.R. Pater⁸², S. Patricelli^{102a,102b}, T. Pauly³⁰, M. Pecsny^{144a}, S. Pedraza Lopez¹⁶⁷, M.I. Pedraza Morales¹⁷³, S.V. Peleganchuk¹⁰⁷, D. Pelikan¹⁶⁶, H. Peng^{33b}, B. Penning³¹, A. Penson³⁵, J. Penwell⁶⁰, M. Perantoni^{24a}, K. Perez^{35,af}, T. Perez Cavalcanti⁴², E. Perez Codina^{159a}, M.T. Pérez García-Estañ¹⁶⁷, V. Perez Reale³⁵, L. Perini^{89a,89b}, H. Pernegger³⁰, R. Perrino^{72a}, P. Perrodo⁵, V.D. Peshekhonov⁶⁴, K. Peters³⁰, B.A. Petersen³⁰, J. Petersen³⁰, T.C. Petersen³⁶,

E. Petit⁵, A. Petridis¹⁵⁴, C. Petridou¹⁵⁴, E. Petrolo^{132a}, F. Petrucci^{134a,134b}, D. Petschull⁴²,
 M. Petteni¹⁴², R. Pezoa^{32b}, A. Phan⁸⁶, P.W. Phillips¹²⁹, G. Piacquadio³⁰, A. Picazio⁴⁹,
 E. Piccaro⁷⁵, M. Piccinini^{20a,20b}, S.M. Piec⁴², R. Piegai²⁷, D.T. Pignotti¹⁰⁹, J.E. Pilcher³¹,
 A.D. Pilkington⁸², J. Pina^{124a,c}, M. Pinamonti^{164a,164c}, A. Pinder¹¹⁸, J.L. Pinfeld³, A. Pingel³⁶,
 B. Pinto^{124a}, C. Pizio^{89a,89b}, M.-A. Pleier²⁵, E. Plotnikova⁶⁴, A. Poblaguev²⁵, S. Poddar^{58a},
 F. Podlyski³⁴, L. Poggioli¹¹⁵, D. Pohl²¹, M. Pohl⁴⁹, G. Polesello^{119a}, A. Policicchio^{37a,37b},
 A. Polini^{20a}, J. Poll⁷⁵, V. Polychronakos²⁵, D. Pomeroy²³, K. Pommès³⁰, L. Pontecorvo^{132a},
 B.G. Pope⁸⁸, G.A. Popeneciu^{26a}, D.S. Popovic^{13a}, A. Poppleton³⁰, X. Portell Bueso³⁰,
 G.E. Pospelov⁹⁹, S. Pospisil¹²⁶, I.N. Potrap⁹⁹, C.J. Potter¹⁴⁹, C.T. Potter¹¹⁴, G. Poulard³⁰,
 J. Poveda⁶⁰, V. Pozdnyakov⁶⁴, R. Prabhu⁷⁷, P. Pralavorio⁸³, A. Pranko¹⁵, S. Prasad³⁰,
 R. Pravahan²⁵, S. Prell⁶³, K. Pretzl¹⁷, D. Price⁶⁰, J. Price⁷³, L.E. Price⁶, D. Prieur¹²³,
 M. Primavera^{72a}, K. Prokofiev¹⁰⁸, F. Prokoshin^{32b}, S. Protopopescu²⁵, J. Proudfoot⁶, X. Prudent⁴⁴,
 M. Przybycien³⁸, H. Przysieznik⁵, S. Psoroulas²¹, E. Ptacek¹¹⁴, E. Pueschel⁸⁴, D. Puldon¹⁴⁸,
 J. Purdham⁸⁷, M. Purohit^{25,ad}, P. Puzo¹¹⁵, Y. Pylypchenko⁶², J. Qian⁸⁷, A. Quadri⁵⁴,
 D.R. Quarrie¹⁵, W.B. Quayle¹⁷³, M. Raas¹⁰⁴, V. Radeka²⁵, V. Radescu⁴², P. Radloff¹¹⁴,
 F. Ragusa^{89a,89b}, G. Rahal¹⁷⁸, A.M. Rahimi¹⁰⁹, D. Rahm²⁵, S. Rajagopalan²⁵, M. Rammensee⁴⁸,
 M. Rammes¹⁴¹, A.S. Randle-Conde⁴⁰, K. Randrianarivony²⁹, K. Rao¹⁶³, F. Rauscher⁹⁸,
 T.C. Rave⁴⁸, M. Raymond³⁰, A.L. Read¹¹⁷, D.M. Rebutti^{119a,119b}, A. Redelbach¹⁷⁴,
 G. Redlinger²⁵, R. Reece¹²⁰, K. Reeves⁴¹, A. Reinsch¹¹⁴, I. Reisinger⁴³, C. Rembser³⁰,
 Z.L. Ren¹⁵¹, A. Renaud¹¹⁵, M. Rescigno^{132a}, S. Resconi^{89a}, B. Resende¹³⁶, P. Reznicek⁹⁸,
 R. Rezvani¹⁵⁸, R. Richter⁹⁹, E. Richter-Was^{5,ag}, M. Ridel⁷⁸, M. Rijpstra¹⁰⁵, M. Rijssenbeek¹⁴⁸,
 A. Rimoldi^{119a,119b}, L. Rinaldi^{20a}, R.R. Rios⁴⁰, I. Riu¹², G. Rivoltella^{89a,89b}, F. Rizatdinova¹¹²,
 E. Rizvi⁷⁵, S.H. Robertson^{85,l}, A. Robichaud-Veronneau¹¹⁸, D. Robinson²⁸, J.E.M. Robinson⁸²,
 A. Robson⁵³, J.G. Rocha de Lima¹⁰⁶, C. Roda^{122a,122b}, D. Roda Dos Santos³⁰, A. Roe⁵⁴, S. Roe³⁰,
 O. Røhne¹¹⁷, S. Rolli¹⁶¹, A. Romaniouk⁹⁶, M. Romano^{20a,20b}, G. Romeo²⁷, E. Romero Adam¹⁶⁷,
 N. Rompotis¹³⁸, L. Roos⁷⁸, E. Ros¹⁶⁷, S. Rosati^{132a}, K. Rosbach⁴⁹, A. Rose¹⁴⁹, M. Rose⁷⁶,
 G.A. Rosenbaum¹⁵⁸, P.L. Rosendahl¹⁴, O. Rosenthal¹⁴¹, L. Rosselet⁴⁹, V. Rossetti¹²,
 E. Rossi^{132a,132b}, L.P. Rossi^{50a}, M. Rotaru^{26a}, I. Roth¹⁷², J. Rothberg¹³⁸, D. Rousseau¹¹⁵,
 C.R. Royon¹³⁶, A. Rozanov⁸³, Y. Rozen¹⁵², X. Ruan^{33a,ah}, F. Rubbo¹², I. Rubinskiy⁴²,
 N. Ruckstuhl¹⁰⁵, V.I. Rud⁹⁷, C. Rudolph⁴⁴, G. Rudolph⁶¹, F. Rühr⁷, A. Ruiz-Martinez⁶³,
 L. Rummyantsev⁶⁴, Z. Rurikova⁴⁸, N.A. Rusakovich⁶⁴, A. Ruschke⁹⁸, J.P. Rutherford⁷,
 N. Ruthmann⁴⁸, P. Ruzicka¹²⁵, Y.F. Ryabov¹²¹, M. Rybar¹²⁷, G. Rybkin¹¹⁵, N.C. Ryder¹¹⁸,
 A.F. Saavedra¹⁵⁰, I. Sadeh¹⁵³, H.F.W. Sadrozinski¹³⁷, R. Sadykov⁶⁴, F. Safai Tehrani^{132a},
 H. Sakamoto¹⁵⁵, G. Salamanna⁷⁵, A. Salamon^{133a}, M. Saleem¹¹¹, D. Salek³⁰, D. Salihagic⁹⁹,
 A. Salmikov¹⁴³, J. Salt¹⁶⁷, B.M. Salvachua Ferrando⁶, D. Salvatore^{37a,37b}, F. Salvatore¹⁴⁹,
 A. Salvucci¹⁰⁴, A. Salzburger³⁰, D. Sampsonidis¹⁵⁴, B.H. Samset¹¹⁷, A. Sanchez^{102a,102b},
 V. Sanchez Martinez¹⁶⁷, H. Sandaker¹⁴, H.G. Sander⁸¹, M.P. Sanders⁹⁸, M. Sandhoff¹⁷⁵,
 T. Sandoval²⁸, C. Sandoval¹⁶², R. Sandstroem⁹⁹, D.P.C. Sankey¹²⁹, A. Sansoni⁴⁷,
 C. Santamarina Rios⁸⁵, C. Santoni³⁴, R. Santonico^{133a,133b}, H. Santos^{124a}, I. Santoyo Castillo¹⁴⁹,
 J.G. Saraiva^{124a}, T. Sarangi¹⁷³, E. Sarkisyan-Grinbaum⁸, B. Sarrazin²¹, F. Sarri^{122a,122b},
 G. Sartiso¹⁷⁵, O. Sasaki⁶⁵, Y. Sasaki¹⁵⁵, N. Sasao⁶⁷, I. Satsounkevitch⁹⁰, G. Sauvage^{5,*},
 E. Sauvan⁵, J.B. Sauvan¹¹⁵, P. Savard^{158,f}, V. Savinov¹²³, D.O. Savu³⁰, L. Sawyer^{25,n},
 D.H. Saxon⁵³, J. Saxon¹²⁰, C. Sbarra^{20a}, A. Sbrizzi^{20a,20b}, D.A. Scannicchio¹⁶³, M. Scarella¹⁵⁰,

J. Schaarschmidt¹¹⁵, P. Schacht⁹⁹, D. Schaefer¹²⁰, U. Schäfer⁸¹, A. Schaelicke⁴⁶, S. Schaepe²¹, S. Schaetzel^{58b}, A.C. Schaffer¹¹⁵, D. Schaile⁹⁸, R.D. Schamberger¹⁴⁸, A.G. Schamov¹⁰⁷, V. Scharf^{58a}, V.A. Schegelsky¹²¹, D. Scheirich⁸⁷, M. Schernau¹⁶³, M.I. Scherzer³⁵, C. Schiavi^{50a,50b}, J. Schieck⁹⁸, M. Schioppa^{37a,37b}, S. Schlenker³⁰, E. Schmidt⁴⁸, K. Schmieden²¹, C. Schmitt⁸¹, S. Schmitt^{58b}, B. Schneider¹⁷, U. Schnoor⁴⁴, L. Schoeffel¹³⁶, A. Schoening^{58b}, A.L.S. Schorlemmer⁵⁴, M. Schott³⁰, D. Schouten^{159a}, J. Schovancova¹²⁵, M. Schram⁸⁵, C. Schroeder⁸¹, N. Schroer^{58c}, M.J. Schultens²¹, J. Schultes¹⁷⁵, H.-C. Schultz-Coulon^{58a}, H. Schulz¹⁶, M. Schumacher⁴⁸, B.A. Schumm¹³⁷, Ph. Schune¹³⁶, A. Schwartzman¹⁴³, Ph. Schwegler⁹⁹, Ph. Schwemling⁷⁸, R. Schwienhorst⁸⁸, R. Schwierz⁴⁴, J. Schwindling¹³⁶, T. Schwindt²¹, M. Schwoerer⁵, F.G. Sciacca¹⁷, G. Sciolla²³, W.G. Scott¹²⁹, J. Searcy¹¹⁴, G. Sedov⁴², E. Sedykh¹²¹, S.C. Seidel¹⁰³, A. Seiden¹³⁷, F. Seifert⁴⁴, J.M. Seixas^{24a}, G. Sekhniaidze^{102a}, S.J. Sekula⁴⁰, K.E. Selbach⁴⁶, D.M. Seliverstov¹²¹, B. Sellden^{146a}, G. Sellers⁷³, M. Seman^{144b}, N. Semprini-Cesari^{20a,20b}, C. Serfon⁹⁸, L. Serin¹¹⁵, L. Serkin⁵⁴, R. Seuster^{159a}, H. Severini¹¹¹, A. Sfyrla³⁰, E. Shabalina⁵⁴, M. Shamim¹¹⁴, L.Y. Shan^{33a}, J.T. Shank²², Q.T. Shao⁸⁶, M. Shapiro¹⁵, P.B. Shatalov⁹⁵, K. Shaw^{164a,164c}, D. Sherman¹⁷⁶, P. Sherwood⁷⁷, S. Shimizu¹⁰¹, M. Shimojima¹⁰⁰, T. Shin⁵⁶, M. Shiyakova⁶⁴, A. Shmeleva⁹⁴, M.J. Shochet³¹, D. Short¹¹⁸, S. Shrestha⁶³, E. Shulga⁹⁶, M.A. Shupe⁷, P. Sicho¹²⁵, A. Sidoti^{132a}, F. Siegert⁴⁸, Dj. Sijacki^{13a}, O. Silbert¹⁷², J. Silva^{124a}, Y. Silver¹⁵³, D. Silverstein¹⁴³, S.B. Silverstein^{146a}, V. Simak¹²⁶, O. Simard¹³⁶, Lj. Simic^{13a}, S. Simion¹¹⁵, E. Simioni⁸¹, B. Simmons⁷⁷, R. Simoniello^{89a,89b}, M. Simonyan³⁶, P. Sinervo¹⁵⁸, N.B. Sinev¹¹⁴, V. Sipica¹⁴¹, G. Siragusa¹⁷⁴, A. Sircar²⁵, A.N. Sisakyan^{64,*}, S.Yu. Sivoklokov⁹⁷, J. Sjölin^{146a,146b}, T.B. Sjrursen¹⁴, L.A. Skinnari¹⁵, H.P. Skottowe⁵⁷, K. Skovpen¹⁰⁷, P. Skubic¹¹¹, M. Slater¹⁸, T. Slavicek¹²⁶, K. Sliwa¹⁶¹, V. Smakhtin¹⁷², B.H. Smart⁴⁶, L. Smestad¹¹⁷, S.Yu. Smirnov⁹⁶, Y. Smirnov⁹⁶, L.N. Smirnova⁹⁷, O. Smirnova⁷⁹, B.C. Smith⁵⁷, D. Smith¹⁴³, K.M. Smith⁵³, M. Smizanska⁷¹, K. Smolek¹²⁶, A.A. Snesarev⁹⁴, S.W. Snow⁸², J. Snow¹¹¹, S. Snyder²⁵, R. Sobie^{169,l}, J. Sodomka¹²⁶, A. Soffer¹⁵³, C.A. Solans¹⁶⁷, M. Solar¹²⁶, J. Solc¹²⁶, E.Yu. Soldatov⁹⁶, U. Soldevila¹⁶⁷, E. Solfaroli Camillocci^{132a,132b}, A.A. Solodkov¹²⁸, O.V. Solovyanov¹²⁸, V. Solovyev¹²¹, N. Soni¹, A. Sood¹⁵, V. Sopko¹²⁶, B. Sopko¹²⁶, M. Sosebee⁸, R. Soualah^{164a,164c}, P. Soueid⁹³, A. Soukharev¹⁰⁷, S. Spagnolo^{72a,72b}, F. Spanò⁷⁶, R. Spighi^{20a}, G. Spigo³⁰, R. Spiwoks³⁰, M. Spousta^{127,ai}, T. Spreitzer¹⁵⁸, B. Spurlock⁸, R.D. St. Denis⁵³, J. Stahlman¹²⁰, R. Stamen^{58a}, E. Stanecka³⁹, R.W. Stanek⁶, C. Stanescu^{134a}, M. Stanescu-Bellu⁴², M.M. Stanitzki⁴², S. Stapnes¹¹⁷, E.A. Starchenko¹²⁸, J. Stark⁵⁵, P. Staroba¹²⁵, P. Starovoitov⁴², R. Staszewski³⁹, A. Staude⁹⁸, P. Stavina^{144a,*}, G. Steele⁵³, P. Steinbach⁴⁴, P. Steinberg²⁵, I. Stekl¹²⁶, B. Stelzer¹⁴², H.J. Stelzer⁸⁸, O. Stelzer-Chilton^{159a}, H. Stenzel⁵², S. Stern⁹⁹, G.A. Stewart³⁰, J.A. Stillings²¹, M.C. Stockton⁸⁵, K. Stoerig⁴⁸, G. Stoicea^{26a}, S. Stonjek⁹⁹, P. Strachota¹²⁷, A.R. Stradling⁸, A. Straessner⁴⁴, J. Strandberg¹⁴⁷, S. Strandberg^{146a,146b}, A. Strandlie¹¹⁷, M. Strang¹⁰⁹, E. Strauss¹⁴³, M. Strauss¹¹¹, P. Strizenec^{144b}, R. Ströhmer¹⁷⁴, D.M. Strom¹¹⁴, J.A. Strong^{76,*}, R. Stroynowski⁴⁰, B. Stugu¹⁴, I. Stumer^{25,*}, J. Stupak¹⁴⁸, P. Sturm¹⁷⁵, N.A. Styles⁴², D.A. Soh^{151,v}, D. Su¹⁴³, HS. Subramania³, R. Subramaniam²⁵, A. Succurro¹², Y. Sugaya¹¹⁶, C. Suhr¹⁰⁶, M. Suk¹²⁷, V.V. Sulin⁹⁴, S. Sultansoy^{4d}, T. Sumida⁶⁷, X. Sun⁵⁵, J.E. Sundermann⁴⁸, K. Suruliz¹³⁹, G. Susinno^{37a,37b}, M.R. Sutton¹⁴⁹, Y. Suzuki⁶⁵, Y. Suzuki⁶⁶, M. Svatos¹²⁵, S. Swedish¹⁶⁸, I. Sykora^{144a}, T. Sykora¹²⁷, J. Sánchez¹⁶⁷, D. Ta¹⁰⁵, K. Tackmann⁴², A. Taffard¹⁶³, R. Tafirout^{159a}, N. Taiblum¹⁵³, Y. Takahashi¹⁰¹, H. Takai²⁵,

R. Takashima⁶⁸, H. Takeda⁶⁶, T. Takeshita¹⁴⁰, Y. Takubo⁶⁵, M. Talby⁸³, A. Talyshev^{107,h}, M.C. Tamsett²⁵, K.G. Tan⁸⁶, J. Tanaka¹⁵⁵, R. Tanaka¹¹⁵, S. Tanaka¹³¹, S. Tanaka⁶⁵, A.J. Tanasijczuk¹⁴², K. Tani⁶⁶, N. Tannoury⁸³, S. Tapprogge⁸¹, D. Tardif¹⁵⁸, S. Tarem¹⁵², F. Tarrade²⁹, G.F. Tartarelli^{89a}, P. Tas¹²⁷, M. Tasevsky¹²⁵, E. Tassi^{37a,37b}, Y. Tayalati^{135d}, C. Taylor⁷⁷, F.E. Taylor⁹², G.N. Taylor⁸⁶, W. Taylor^{159b}, M. Teinturier¹¹⁵, F.A. Teischinger³⁰, M. Teixeira Dias Castanheira⁷⁵, P. Teixeira-Dias⁷⁶, K.K. Temming⁴⁸, H. Ten Kate³⁰, P.K. Teng¹⁵¹, S. Terada⁶⁵, K. Terashi¹⁵⁵, J. Terron⁸⁰, M. Testa⁴⁷, R.J. Teuscher^{158,l}, J. Therhaag²¹, T. Theveneaux-Pelzer⁷⁸, S. Thoma⁴⁸, J.P. Thomas¹⁸, E.N. Thompson³⁵, P.D. Thompson¹⁸, P.D. Thompson¹⁵⁸, A.S. Thompson⁵³, L.A. Thomsen³⁶, E. Thomson¹²⁰, M. Thomson²⁸, W.M. Thong⁸⁶, R.P. Thun⁸⁷, F. Tian³⁵, M.J. Tibbetts¹⁵, T. Tic¹²⁵, V.O. Tikhomirov⁹⁴, Y.A. Tikhonov^{107,h}, S. Timoshenko⁹⁶, E. Tiouchichine⁸³, P. Tipton¹⁷⁶, S. Tisserant⁸³, T. Todorov⁵, S. Todorova-Nova¹⁶¹, B. Toggerson¹⁶³, J. Tojo⁶⁹, S. Tokár^{144a}, K. Tokushuku⁶⁵, K. Tollefson⁸⁸, M. Tomoto¹⁰¹, L. Tompkins³¹, K. Toms¹⁰³, A. Tonoyan¹⁴, C. Topfel¹⁷, N.D. Topilin⁶⁴, E. Torrence¹¹⁴, H. Torres⁷⁸, E. Torró Pastor¹⁶⁷, J. Toth^{83,ae}, F. Touchard⁸³, D.R. Tovey¹³⁹, T. Trefzger¹⁷⁴, L. Tremblet³⁰, A. Tricoli³⁰, I.M. Trigger^{159a}, S. Trincaz-Duvoid⁷⁸, M.F. Tripiana⁷⁰, N. Triplett²⁵, W. Trischuk¹⁵⁸, B. Trocmé⁵⁵, C. Troncon^{89a}, M. Trotter-McDonald¹⁴², P. True⁸⁸, M. Trzebinski³⁹, A. Trzupke³⁹, C. Tsarouchas³⁰, J.C-L. Tseng¹¹⁸, M. Tsiakiris¹⁰⁵, P.V. Tsiareshka⁹⁰, D. Tsionou^{5,aj}, G. Tsipolitis¹⁰, S. Tsiskaridze¹², V. Tsiskaridze⁴⁸, E.G. Tskhadadze^{51a}, I.I. Tsukerman⁹⁵, V. Tsulaia¹⁵, J.-W. Tsung²¹, S. Tsuno⁶⁵, D. Tsybychev¹⁴⁸, A. Tua¹³⁹, A. Tudorache^{26a}, V. Tudorache^{26a}, J.M. Tuggle³¹, M. Turala³⁹, D. Turecek¹²⁶, I. Turk Cakir^{4e}, E. Turlay¹⁰⁵, R. Turra^{89a,89b}, P.M. Tuts³⁵, A. Tykhonov⁷⁴, M. Tylmad^{146a,146b}, M. Tyndel¹²⁹, G. Tzanakos⁹, K. Uchida²¹, I. Ueda¹⁵⁵, R. Ueno²⁹, M. Ughetto⁸³, M. Ugland¹⁴, M. Uhlenbrock²¹, M. Uhrmacher⁵⁴, F. Ukegawa¹⁶⁰, G. Unal³⁰, A. Undrus²⁵, G. Unel¹⁶³, Y. Unno⁶⁵, D. Urbaniec³⁵, P. Urquijo²¹, G. Usai⁸, M. Uslenghi^{119a,119b}, L. Vacavant⁸³, V. Vacek¹²⁶, B. Vachon⁸⁵, S. Vahsen¹⁵, S. Valentineti^{20a,20b}, A. Valero¹⁶⁷, S. Valkar¹²⁷, E. Valladolid Gallego¹⁶⁷, S. Vallecorsa¹⁵², J.A. Valls Ferrer¹⁶⁷, R. Van Berg¹²⁰, P.C. Van Der Deijl¹⁰⁵, R. van der Geer¹⁰⁵, H. van der Graaf¹⁰⁵, R. Van Der Leeuw¹⁰⁵, E. van der Poel¹⁰⁵, D. van der Ster³⁰, N. van Eldik³⁰, P. van Gemmeren⁶, J. Van Nieuwkoop¹⁴², I. van Vulpen¹⁰⁵, M. Vanadia⁹⁹, W. Vandelli³⁰, A. Vaniachine⁶, P. Vankov⁴², F. Vannucci⁷⁸, R. Vari^{132a}, E.W. Varnes⁷, T. Varol⁸⁴, D. Varouchas¹⁵, A. Vartapetian⁸, K.E. Varvell¹⁵⁰, V.I. Vassilakopoulos⁵⁶, F. Vazeille³⁴, T. Vazquez Schroeder⁵⁴, G. Vegni^{89a,89b}, J.J. Veillet¹¹⁵, F. Veloso^{124a}, R. Veness³⁰, S. Veneziano^{132a}, A. Ventura^{72a,72b}, D. Ventura⁸⁴, M. Venturi⁴⁸, N. Venturi¹⁵⁸, V. Vercesi^{119a}, M. Verducci¹³⁸, W. Verkerke¹⁰⁵, J.C. Vermeulen¹⁰⁵, A. Vest⁴⁴, M.C. Vetterli^{142,f}, I. Vichou¹⁶⁵, T. Vickey^{145b,ak}, O.E. Vickey Boeriu^{145b}, G.H.A. Viehhauser¹¹⁸, S. Viel¹⁶⁸, M. Villa^{20a,20b}, M. Villaplana Perez¹⁶⁷, E. Vilucchi⁴⁷, M.G. Vincter²⁹, E. Vinek³⁰, V.B. Vinogradov⁶⁴, M. Virchaux^{136,*}, J. Virzi¹⁵, O. Vitells¹⁷², M. Viti⁴², I. Vivarelli⁴⁸, F. Vives Vaque³, S. Vlachos¹⁰, D. Vladoiu⁹⁸, M. Vlasak¹²⁶, A. Vogel²¹, P. Vokac¹²⁶, G. Volpi⁴⁷, M. Volpi⁸⁶, G. Volpini^{89a}, H. von der Schmitt⁹⁹, H. von Radziewski⁴⁸, E. von Toerne²¹, V. Vorobel¹²⁷, V. Vorwerk¹², M. Vos¹⁶⁷, R. Voss³⁰, J.H. Vosseveld⁷³, N. Vranjes¹³⁶, M. Vranjes Milosavljevic¹⁰⁵, V. Vrba¹²⁵, M. Vreeswijk¹⁰⁵, T. Vu Anh⁴⁸, R. Vuillermet³⁰, I. Vukotic³¹, W. Wagner¹⁷⁵, P. Wagner²¹, H. Wahlen¹⁷⁵, S. Wahrmond⁴⁴, J. Wakabayashi¹⁰¹, S. Walch⁸⁷, J. Walder⁷¹, R. Walker⁹⁸, W. Walkowiak¹⁴¹, R. Wall¹⁷⁶, P. Waller⁷³, B. Walsh¹⁷⁶, C. Wang⁴⁵, H. Wang¹⁷³, H. Wang⁴⁰, J. Wang¹⁵¹, J. Wang^{33a}, R. Wang¹⁰³, S.M. Wang¹⁵¹,

T. Wang²¹, A. Warburton⁸⁵, C.P. Ward²⁸, D.R. Wardrope⁷⁷, M. Warsinsky⁴⁸, A. Washbrook⁴⁶, C. Wasicki⁴², I. Watanabe⁶⁶, P.M. Watkins¹⁸, A.T. Watson¹⁸, I.J. Watson¹⁵⁰, M.F. Watson¹⁸, G. Watts¹³⁸, S. Watts⁸², A.T. Waugh¹⁵⁰, B.M. Waugh⁷⁷, M.S. Weber¹⁷, J.S. Webster³¹, A.R. Weidberg¹¹⁸, P. Weigell⁹⁹, J. Weingarten⁵⁴, C. Weiser⁴⁸, P.S. Wells³⁰, T. Wenaus²⁵, D. Wendland¹⁶, Z. Weng^{151,v}, T. Wengler³⁰, S. Wenig³⁰, N. Wermes²¹, M. Werner⁴⁸, P. Werner³⁰, M. Werth¹⁶³, M. Wessels^{58a}, J. Wetter¹⁶¹, C. Weydert⁵⁵, K. Whalen²⁹, A. White⁸, M.J. White⁸⁶, S. White^{122a,122b}, S.R. Whitehead¹¹⁸, D. Whiteson¹⁶³, D. Whittington⁶⁰, D. Wicke¹⁷⁵, F.J. Wickens¹²⁹, W. Wiedenmann¹⁷³, M. Wielers¹²⁹, P. Wienemann²¹, C. Wiglesworth⁷⁵, L.A.M. Wiik-Fuchs²¹, P.A. Wijeratne⁷⁷, A. Wildauer⁹⁹, M.A. Wildt^{42,s}, I. Wilhelm¹²⁷, H.G. Wilkens³⁰, J.Z. Will⁹⁸, E. Williams³⁵, H.H. Williams¹²⁰, S. Williams²⁸, W. Willis³⁵, S. Willocq⁸⁴, J.A. Wilson¹⁸, M.G. Wilson¹⁴³, A. Wilson⁸⁷, I. Wingerter-Seez⁵, S. Winkelmann⁴⁸, F. Winklmeier³⁰, M. Wittgen¹⁴³, S.J. Wollstadt⁸¹, M.W. Wolter³⁹, H. Wolters^{124a,i}, W.C. Wong⁴¹, G. Wooden⁸⁷, B.K. Wosiek³⁹, J. Wotschack³⁰, M.J. Woudstra⁸², K.W. Wozniak³⁹, K. Wraight⁵³, M. Wright⁵³, B. Wrona⁷³, S.L. Wu¹⁷³, X. Wu⁴⁹, Y. Wu^{33b,al}, E. Wulf³⁵, B.M. Wynne⁴⁶, S. Xella³⁶, M. Xiao¹³⁶, S. Xie⁴⁸, C. Xu^{33b,z}, D. Xu^{33a}, L. Xu^{33b}, B. Yabsley¹⁵⁰, S. Yacoob^{145a,am}, M. Yamada⁶⁵, H. Yamaguchi¹⁵⁵, A. Yamamoto⁶⁵, K. Yamamoto⁶³, S. Yamamoto¹⁵⁵, T. Yamamura¹⁵⁵, T. Yamanaka¹⁵⁵, T. Yamazaki¹⁵⁵, Y. Yamazaki⁶⁶, Z. Yan²², H. Yang⁸⁷, U.K. Yang⁸², Y. Yang¹⁰⁹, Z. Yang^{146a,146b}, S. Yanush⁹¹, L. Yao^{33a}, Y. Yasu⁶⁵, E. Yatsenko⁴², J. Ye⁴⁰, S. Ye²⁵, A.L. Yen⁵⁷, M. Yilmaz^{4c}, R. Yoosoofmiya¹²³, K. Yorita¹⁷¹, R. Yoshida⁶, K. Yoshihara¹⁵⁵, C. Young¹⁴³, C.J. Young¹¹⁸, S. Youssef²², D. Yu²⁵, D.R. Yu¹⁵, J. Yu⁸, J. Yu¹¹², L. Yuan⁶⁶, A. Yurkewicz¹⁰⁶, B. Zabinski³⁹, R. Zaidan⁶², A.M. Zaitsev¹²⁸, L. Zanello^{132a,132b}, D. Zanzi⁹⁹, A. Zaytsev²⁵, C. Zeitnitz¹⁷⁵, M. Zeman¹²⁶, A. Zemla³⁹, O. Zenin¹²⁸, T. Ženiš^{144a}, Z. Zinonos^{122a,122b}, D. Zerwas¹¹⁵, G. Zevi della Porta⁵⁷, D. Zhang⁸⁷, H. Zhang⁸⁸, J. Zhang⁶, X. Zhang^{33d}, Z. Zhang¹¹⁵, L. Zhao¹⁰⁸, Z. Zhao^{33b}, A. Zhemchugov⁶⁴, J. Zhong¹¹⁸, B. Zhou⁸⁷, N. Zhou¹⁶³, Y. Zhou¹⁵¹, C.G. Zhu^{33d}, H. Zhu⁴², J. Zhu⁸⁷, Y. Zhu^{33b}, X. Zhuang⁹⁸, V. Zhuravlov⁹⁹, A. Zibell⁹⁸, D. Zieminska⁶⁰, N.I. Zimin⁶⁴, R. Zimmermann²¹, S. Zimmermann²¹, S. Zimmermann⁴⁸, M. Ziolkowski¹⁴¹, R. Zitoun⁵, L. Živković³⁵, V.V. Zmouchko^{128,*}, G. Zobernig¹⁷³, A. Zoccoli^{20a,20b}, M. zur Nedden¹⁶, V. Zutshi¹⁰⁶, L. Zwalinski³⁰.

¹ School of Chemistry and Physics, University of Adelaide, Adelaide, Australia

² Physics Department, SUNY Albany, Albany NY, United States of America

³ Department of Physics, University of Alberta, Edmonton AB, Canada

⁴ (a) Department of Physics, Ankara University, Ankara; (b) Department of Physics, Dumlupinar University, Kutahya; (c) Department of Physics, Gazi University, Ankara; (d) Division of Physics, TOBB University of Economics and Technology, Ankara; (e) Turkish Atomic Energy Authority, Ankara, Turkey

⁵ LAPP, CNRS/IN2P3 and Université de Savoie, Annecy-le-Vieux, France

⁶ High Energy Physics Division, Argonne National Laboratory, Argonne IL, United States of America

⁷ Department of Physics, University of Arizona, Tucson AZ, United States of America

⁸ Department of Physics, The University of Texas at Arlington, Arlington TX, United States of America

⁹ Physics Department, University of Athens, Athens, Greece

- ¹⁰ Physics Department, National Technical University of Athens, Zografou, Greece
- ¹¹ Institute of Physics, Azerbaijan Academy of Sciences, Baku, Azerbaijan
- ¹² Institut de Física d'Altes Energies and Departament de Física de la Universitat Autònoma de Barcelona and ICREA, Barcelona, Spain
- ¹³ ^(a) Institute of Physics, University of Belgrade, Belgrade; ^(b) Vinca Institute of Nuclear Sciences, University of Belgrade, Belgrade, Serbia
- ¹⁴ Department for Physics and Technology, University of Bergen, Bergen, Norway
- ¹⁵ Physics Division, Lawrence Berkeley National Laboratory and University of California, Berkeley CA, United States of America
- ¹⁶ Department of Physics, Humboldt University, Berlin, Germany
- ¹⁷ Albert Einstein Center for Fundamental Physics and Laboratory for High Energy Physics, University of Bern, Bern, Switzerland
- ¹⁸ School of Physics and Astronomy, University of Birmingham, Birmingham, United Kingdom
- ¹⁹ ^(a) Department of Physics, Bogazici University, Istanbul; ^(b) Division of Physics, Dogus University, Istanbul; ^(c) Department of Physics Engineering, Gaziantep University, Gaziantep; ^(d) Department of Physics, Istanbul Technical University, Istanbul, Turkey
- ²⁰ ^(a) INFN Sezione di Bologna; ^(b) Dipartimento di Fisica, Università di Bologna, Bologna, Italy
- ²¹ Physikalisches Institut, University of Bonn, Bonn, Germany
- ²² Department of Physics, Boston University, Boston MA, United States of America
- ²³ Department of Physics, Brandeis University, Waltham MA, United States of America
- ²⁴ ^(a) Universidade Federal do Rio De Janeiro COPPE/EE/IF, Rio de Janeiro; ^(b) Federal University of Juiz de Fora (UFJF), Juiz de Fora; ^(c) Federal University of Sao Joao del Rei (UFSJ), Sao Joao del Rei; ^(d) Instituto de Fisica, Universidade de Sao Paulo, Sao Paulo, Brazil
- ²⁵ Physics Department, Brookhaven National Laboratory, Upton NY, United States of America
- ²⁶ ^(a) National Institute of Physics and Nuclear Engineering, Bucharest; ^(b) University Politehnica Bucharest, Bucharest; ^(c) West University in Timisoara, Timisoara, Romania
- ²⁷ Departamento de Física, Universidad de Buenos Aires, Buenos Aires, Argentina
- ²⁸ Cavendish Laboratory, University of Cambridge, Cambridge, United Kingdom
- ²⁹ Department of Physics, Carleton University, Ottawa ON, Canada
- ³⁰ CERN, Geneva, Switzerland
- ³¹ Enrico Fermi Institute, University of Chicago, Chicago IL, United States of America
- ³² ^(a) Departamento de Física, Pontificia Universidad Católica de Chile, Santiago; ^(b) Departamento de Física, Universidad Técnica Federico Santa María, Valparaíso, Chile
- ³³ ^(a) Institute of High Energy Physics, Chinese Academy of Sciences, Beijing; ^(b) Department of Modern Physics, University of Science and Technology of China, Anhui; ^(c) Department of Physics, Nanjing University, Jiangsu; ^(d) School of Physics, Shandong University, Shandong; ^(e) Physics Department, Shanghai Jiao Tong University, Shanghai, China
- ³⁴ Laboratoire de Physique Corpusculaire, Clermont Université and Université Blaise Pascal and CNRS/IN2P3, Clermont-Ferrand, France
- ³⁵ Nevis Laboratory, Columbia University, Irvington NY, United States of America
- ³⁶ Niels Bohr Institute, University of Copenhagen, Kobenhavn, Denmark
- ³⁷ ^(a) INFN Gruppo Collegato di Cosenza; ^(b) Dipartimento di Fisica, Università della Calabria, Arcavata di Rende, Italy

- ³⁸ AGH University of Science and Technology, Faculty of Physics and Applied Computer Science, Krakow, Poland
- ³⁹ The Henryk Niewodniczanski Institute of Nuclear Physics, Polish Academy of Sciences, Krakow, Poland
- ⁴⁰ Physics Department, Southern Methodist University, Dallas TX, United States of America
- ⁴¹ Physics Department, University of Texas at Dallas, Richardson TX, United States of America
- ⁴² DESY, Hamburg and Zeuthen, Germany
- ⁴³ Institut für Experimentelle Physik IV, Technische Universität Dortmund, Dortmund, Germany
- ⁴⁴ Institut für Kern- und Teilchenphysik, Technical University Dresden, Dresden, Germany
- ⁴⁵ Department of Physics, Duke University, Durham NC, United States of America
- ⁴⁶ SUPA - School of Physics and Astronomy, University of Edinburgh, Edinburgh, United Kingdom
- ⁴⁷ INFN Laboratori Nazionali di Frascati, Frascati, Italy
- ⁴⁸ Fakultät für Mathematik und Physik, Albert-Ludwigs-Universität, Freiburg, Germany
- ⁴⁹ Section de Physique, Université de Genève, Geneva, Switzerland
- ⁵⁰ ^(a) INFN Sezione di Genova; ^(b) Dipartimento di Fisica, Università di Genova, Genova, Italy
- ⁵¹ ^(a) E. Andronikashvili Institute of Physics, Iv. Javakhishvili Tbilisi State University, Tbilisi; ^(b) High Energy Physics Institute, Tbilisi State University, Tbilisi, Georgia
- ⁵² II Physikalisches Institut, Justus-Liebig-Universität Giessen, Giessen, Germany
- ⁵³ SUPA - School of Physics and Astronomy, University of Glasgow, Glasgow, United Kingdom
- ⁵⁴ II Physikalisches Institut, Georg-August-Universität, Göttingen, Germany
- ⁵⁵ Laboratoire de Physique Subatomique et de Cosmologie, Université Joseph Fourier and CNRS/IN2P3 and Institut National Polytechnique de Grenoble, Grenoble, France
- ⁵⁶ Department of Physics, Hampton University, Hampton VA, United States of America
- ⁵⁷ Laboratory for Particle Physics and Cosmology, Harvard University, Cambridge MA, United States of America
- ⁵⁸ ^(a) Kirchhoff-Institut für Physik, Ruprecht-Karls-Universität Heidelberg, Heidelberg; ^(b) Physikalisches Institut, Ruprecht-Karls-Universität Heidelberg, Heidelberg; ^(c) ZITI Institut für technische Informatik, Ruprecht-Karls-Universität Heidelberg, Mannheim, Germany
- ⁵⁹ Faculty of Applied Information Science, Hiroshima Institute of Technology, Hiroshima, Japan
- ⁶⁰ Department of Physics, Indiana University, Bloomington IN, United States of America
- ⁶¹ Institut für Astro- und Teilchenphysik, Leopold-Franzens-Universität, Innsbruck, Austria
- ⁶² University of Iowa, Iowa City IA, United States of America
- ⁶³ Department of Physics and Astronomy, Iowa State University, Ames IA, United States of America
- ⁶⁴ Joint Institute for Nuclear Research, JINR Dubna, Dubna, Russia
- ⁶⁵ KEK, High Energy Accelerator Research Organization, Tsukuba, Japan
- ⁶⁶ Graduate School of Science, Kobe University, Kobe, Japan
- ⁶⁷ Faculty of Science, Kyoto University, Kyoto, Japan
- ⁶⁸ Kyoto University of Education, Kyoto, Japan
- ⁶⁹ Department of Physics, Kyushu University, Fukuoka, Japan
- ⁷⁰ Instituto de Física La Plata, Universidad Nacional de La Plata and CONICET, La Plata, Argentina

- ⁷¹ Physics Department, Lancaster University, Lancaster, United Kingdom
- ⁷² ^(a) INFN Sezione di Lecce; ^(b) Dipartimento di Matematica e Fisica, Università del Salento, Lecce, Italy
- ⁷³ Oliver Lodge Laboratory, University of Liverpool, Liverpool, United Kingdom
- ⁷⁴ Department of Physics, Jožef Stefan Institute and University of Ljubljana, Ljubljana, Slovenia
- ⁷⁵ School of Physics and Astronomy, Queen Mary University of London, London, United Kingdom
- ⁷⁶ Department of Physics, Royal Holloway University of London, Surrey, United Kingdom
- ⁷⁷ Department of Physics and Astronomy, University College London, London, United Kingdom
- ⁷⁸ Laboratoire de Physique Nucléaire et de Hautes Energies, UPMC and Université Paris-Diderot and CNRS/IN2P3, Paris, France
- ⁷⁹ Fysiska institutionen, Lunds universitet, Lund, Sweden
- ⁸⁰ Departamento de Física Teórica C-15, Universidad Autónoma de Madrid, Madrid, Spain
- ⁸¹ Institut für Physik, Universität Mainz, Mainz, Germany
- ⁸² School of Physics and Astronomy, University of Manchester, Manchester, United Kingdom
- ⁸³ CPPM, Aix-Marseille Université and CNRS/IN2P3, Marseille, France
- ⁸⁴ Department of Physics, University of Massachusetts, Amherst MA, United States of America
- ⁸⁵ Department of Physics, McGill University, Montreal QC, Canada
- ⁸⁶ School of Physics, University of Melbourne, Victoria, Australia
- ⁸⁷ Department of Physics, The University of Michigan, Ann Arbor MI, United States of America
- ⁸⁸ Department of Physics and Astronomy, Michigan State University, East Lansing MI, United States of America
- ⁸⁹ ^(a) INFN Sezione di Milano; ^(b) Dipartimento di Fisica, Università di Milano, Milano, Italy
- ⁹⁰ B.I. Stepanov Institute of Physics, National Academy of Sciences of Belarus, Minsk, Republic of Belarus
- ⁹¹ National Scientific and Educational Centre for Particle and High Energy Physics, Minsk, Republic of Belarus
- ⁹² Department of Physics, Massachusetts Institute of Technology, Cambridge MA, United States of America
- ⁹³ Group of Particle Physics, University of Montreal, Montreal QC, Canada
- ⁹⁴ P.N. Lebedev Institute of Physics, Academy of Sciences, Moscow, Russia
- ⁹⁵ Institute for Theoretical and Experimental Physics (ITEP), Moscow, Russia
- ⁹⁶ Moscow Engineering and Physics Institute (MEPhI), Moscow, Russia
- ⁹⁷ Skobeltsyn Institute of Nuclear Physics, Lomonosov Moscow State University, Moscow, Russia
- ⁹⁸ Fakultät für Physik, Ludwig-Maximilians-Universität München, München, Germany
- ⁹⁹ Max-Planck-Institut für Physik (Werner-Heisenberg-Institut), München, Germany
- ¹⁰⁰ Nagasaki Institute of Applied Science, Nagasaki, Japan
- ¹⁰¹ Graduate School of Science and Kobayashi-Maskawa Institute, Nagoya University, Nagoya, Japan
- ¹⁰² ^(a) INFN Sezione di Napoli; ^(b) Dipartimento di Scienze Fisiche, Università di Napoli, Napoli, Italy
- ¹⁰³ Department of Physics and Astronomy, University of New Mexico, Albuquerque NM, United States of America

- ¹⁰⁴ Institute for Mathematics, Astrophysics and Particle Physics, Radboud University Nijmegen/Nikhef, Nijmegen, Netherlands
- ¹⁰⁵ Nikhef National Institute for Subatomic Physics and University of Amsterdam, Amsterdam, Netherlands
- ¹⁰⁶ Department of Physics, Northern Illinois University, DeKalb IL, United States of America
- ¹⁰⁷ Budker Institute of Nuclear Physics, SB RAS, Novosibirsk, Russia
- ¹⁰⁸ Department of Physics, New York University, New York NY, United States of America
- ¹⁰⁹ Ohio State University, Columbus OH, United States of America
- ¹¹⁰ Faculty of Science, Okayama University, Okayama, Japan
- ¹¹¹ Homer L. Dodge Department of Physics and Astronomy, University of Oklahoma, Norman OK, United States of America
- ¹¹² Department of Physics, Oklahoma State University, Stillwater OK, United States of America
- ¹¹³ Palacký University, RCPTM, Olomouc, Czech Republic
- ¹¹⁴ Center for High Energy Physics, University of Oregon, Eugene OR, United States of America
- ¹¹⁵ LAL, Université Paris-Sud and CNRS/IN2P3, Orsay, France
- ¹¹⁶ Graduate School of Science, Osaka University, Osaka, Japan
- ¹¹⁷ Department of Physics, University of Oslo, Oslo, Norway
- ¹¹⁸ Department of Physics, Oxford University, Oxford, United Kingdom
- ¹¹⁹ ^(a) INFN Sezione di Pavia; ^(b) Dipartimento di Fisica, Università di Pavia, Pavia, Italy
- ¹²⁰ Department of Physics, University of Pennsylvania, Philadelphia PA, United States of America
- ¹²¹ Petersburg Nuclear Physics Institute, Gatchina, Russia
- ¹²² ^(a) INFN Sezione di Pisa; ^(b) Dipartimento di Fisica E. Fermi, Università di Pisa, Pisa, Italy
- ¹²³ Department of Physics and Astronomy, University of Pittsburgh, Pittsburgh PA, United States of America
- ¹²⁴ ^(a) Laboratório de Instrumentação e Física Experimental de Partículas - LIP, Lisboa, Portugal; ^(b) Departamento de Física Teórica y del Cosmos and CAFPE, Universidad de Granada, Granada, Spain
- ¹²⁵ Institute of Physics, Academy of Sciences of the Czech Republic, Praha, Czech Republic
- ¹²⁶ Czech Technical University in Prague, Praha, Czech Republic
- ¹²⁷ Faculty of Mathematics and Physics, Charles University in Prague, Praha, Czech Republic
- ¹²⁸ State Research Center Institute for High Energy Physics, Protvino, Russia
- ¹²⁹ Particle Physics Department, Rutherford Appleton Laboratory, Didcot, United Kingdom
- ¹³⁰ Physics Department, University of Regina, Regina SK, Canada
- ¹³¹ Ritsumeikan University, Kusatsu, Shiga, Japan
- ¹³² ^(a) INFN Sezione di Roma I; ^(b) Dipartimento di Fisica, Università La Sapienza, Roma, Italy
- ¹³³ ^(a) INFN Sezione di Roma Tor Vergata; ^(b) Dipartimento di Fisica, Università di Roma Tor Vergata, Roma, Italy
- ¹³⁴ ^(a) INFN Sezione di Roma Tre; ^(b) Dipartimento di Fisica, Università Roma Tre, Roma, Italy
- ¹³⁵ ^(a) Faculté des Sciences Ain Chock, Réseau Universitaire de Physique des Hautes Energies - Université Hassan II, Casablanca; ^(b) Centre National de l'Énergie des Sciences Techniques Nucleaires, Rabat; ^(c) Faculté des Sciences Semlalia, Université Cadi Ayyad, LPHEA-Marrakech; ^(d) Faculté des Sciences, Université Mohamed Premier and LPTPM, Oujda; ^(e) Faculté des sciences, Université Mohammed V-Agdal, Rabat, Morocco

- ¹³⁶ DSM/IRFU (Institut de Recherches sur les Lois Fondamentales de l'Univers), CEA Saclay (Commissariat à l'Energie Atomique et aux Energies Alternatives), Gif-sur-Yvette, France
- ¹³⁷ Santa Cruz Institute for Particle Physics, University of California Santa Cruz, Santa Cruz CA, United States of America
- ¹³⁸ Department of Physics, University of Washington, Seattle WA, United States of America
- ¹³⁹ Department of Physics and Astronomy, University of Sheffield, Sheffield, United Kingdom
- ¹⁴⁰ Department of Physics, Shinshu University, Nagano, Japan
- ¹⁴¹ Fachbereich Physik, Universität Siegen, Siegen, Germany
- ¹⁴² Department of Physics, Simon Fraser University, Burnaby BC, Canada
- ¹⁴³ SLAC National Accelerator Laboratory, Stanford CA, United States of America
- ¹⁴⁴ ^(a) Faculty of Mathematics, Physics & Informatics, Comenius University, Bratislava; ^(b) Department of Subnuclear Physics, Institute of Experimental Physics of the Slovak Academy of Sciences, Kosice, Slovak Republic
- ¹⁴⁵ ^(a) Department of Physics, University of Johannesburg, Johannesburg; ^(b) School of Physics, University of the Witwatersrand, Johannesburg, South Africa
- ¹⁴⁶ ^(a) Department of Physics, Stockholm University; ^(b) The Oskar Klein Centre, Stockholm, Sweden
- ¹⁴⁷ Physics Department, Royal Institute of Technology, Stockholm, Sweden
- ¹⁴⁸ Departments of Physics & Astronomy and Chemistry, Stony Brook University, Stony Brook NY, United States of America
- ¹⁴⁹ Department of Physics and Astronomy, University of Sussex, Brighton, United Kingdom
- ¹⁵⁰ School of Physics, University of Sydney, Sydney, Australia
- ¹⁵¹ Institute of Physics, Academia Sinica, Taipei, Taiwan
- ¹⁵² Department of Physics, Technion: Israel Institute of Technology, Haifa, Israel
- ¹⁵³ Raymond and Beverly Sackler School of Physics and Astronomy, Tel Aviv University, Tel Aviv, Israel
- ¹⁵⁴ Department of Physics, Aristotle University of Thessaloniki, Thessaloniki, Greece
- ¹⁵⁵ International Center for Elementary Particle Physics and Department of Physics, The University of Tokyo, Tokyo, Japan
- ¹⁵⁶ Graduate School of Science and Technology, Tokyo Metropolitan University, Tokyo, Japan
- ¹⁵⁷ Department of Physics, Tokyo Institute of Technology, Tokyo, Japan
- ¹⁵⁸ Department of Physics, University of Toronto, Toronto ON, Canada
- ¹⁵⁹ ^(a) TRIUMF, Vancouver BC; ^(b) Department of Physics and Astronomy, York University, Toronto ON, Canada
- ¹⁶⁰ Faculty of Pure and Applied Sciences, University of Tsukuba, Tsukuba, Japan
- ¹⁶¹ Department of Physics and Astronomy, Tufts University, Medford MA, United States of America
- ¹⁶² Centro de Investigaciones, Universidad Antonio Narino, Bogota, Colombia
- ¹⁶³ Department of Physics and Astronomy, University of California Irvine, Irvine CA, United States of America
- ¹⁶⁴ ^(a) INFN Gruppo Collegato di Udine; ^(b) ICTP, Trieste; ^(c) Dipartimento di Chimica, Fisica e Ambiente, Università di Udine, Udine, Italy
- ¹⁶⁵ Department of Physics, University of Illinois, Urbana IL, United States of America

- ¹⁶⁶ Department of Physics and Astronomy, University of Uppsala, Uppsala, Sweden
- ¹⁶⁷ Instituto de Física Corpuscular (IFIC) and Departamento de Física Atómica, Molecular y Nuclear and Departamento de Ingeniería Electrónica and Instituto de Microelectrónica de Barcelona (IMB-CNM), University of Valencia and CSIC, Valencia, Spain
- ¹⁶⁸ Department of Physics, University of British Columbia, Vancouver BC, Canada
- ¹⁶⁹ Department of Physics and Astronomy, University of Victoria, Victoria BC, Canada
- ¹⁷⁰ Department of Physics, University of Warwick, Coventry, United Kingdom
- ¹⁷¹ Waseda University, Tokyo, Japan
- ¹⁷² Department of Particle Physics, The Weizmann Institute of Science, Rehovot, Israel
- ¹⁷³ Department of Physics, University of Wisconsin, Madison WI, United States of America
- ¹⁷⁴ Fakultät für Physik und Astronomie, Julius-Maximilians-Universität, Würzburg, Germany
- ¹⁷⁵ Fachbereich C Physik, Bergische Universität Wuppertal, Wuppertal, Germany
- ¹⁷⁶ Department of Physics, Yale University, New Haven CT, United States of America
- ¹⁷⁷ Yerevan Physics Institute, Yerevan, Armenia
- ¹⁷⁸ Centre de Calcul de l'Institut National de Physique Nucléaire et de Physique des Particules (IN2P3), Villeurbanne, France
- ^a Also at Department of Physics, King's College London, London, United Kingdom
- ^b Also at Laboratório de Instrumentação e Física Experimental de Partículas - LIP, Lisboa, Portugal
- ^c Also at Faculdade de Ciências and CFNUL, Universidade de Lisboa, Lisboa, Portugal
- ^d Also at Particle Physics Department, Rutherford Appleton Laboratory, Didcot, United Kingdom
- ^e Also at Department of Physics, University of Johannesburg, Johannesburg, South Africa
- ^f Also at TRIUMF, Vancouver BC, Canada
- ^g Also at Department of Physics, California State University, Fresno CA, United States of America
- ^h Also at Novosibirsk State University, Novosibirsk, Russia
- ⁱ Also at Department of Physics, University of Coimbra, Coimbra, Portugal
- ^j Also at Department of Physics, UASLP, San Luis Potosi, Mexico
- ^k Also at Università di Napoli Parthenope, Napoli, Italy
- ^l Also at Institute of Particle Physics (IPP), Canada
- ^m Also at Department of Physics, Middle East Technical University, Ankara, Turkey
- ⁿ Also at Louisiana Tech University, Ruston LA, United States of America
- ^o Also at Dep Física and CEFITEC of Faculdade de Ciências e Tecnologia, Universidade Nova de Lisboa, Caparica, Portugal
- ^p Also at Department of Physics and Astronomy, University College London, London, United Kingdom
- ^q Also at Department of Physics, University of Cape Town, Cape Town, South Africa
- ^r Also at Institute of Physics, Azerbaijan Academy of Sciences, Baku, Azerbaijan
- ^s Also at Institut für Experimentalphysik, Universität Hamburg, Hamburg, Germany
- ^t Also at Manhattan College, New York NY, United States of America
- ^u Also at CPPM, Aix-Marseille Université and CNRS/IN2P3, Marseille, France
- ^v Also at School of Physics and Engineering, Sun Yat-sen University, Guanzhou, China
- ^w Also at Academia Sinica Grid Computing, Institute of Physics, Academia Sinica, Taipei, Taiwan
- ^x Also at School of Physics, Shandong University, Shandong, China

^y Also at Dipartimento di Fisica, Università La Sapienza, Roma, Italy

^z Also at DSM/IRFU (Institut de Recherches sur les Lois Fondamentales de l'Univers), CEA Saclay (Commissariat à l'Énergie Atomique et aux Énergies Alternatives), Gif-sur-Yvette, France

^{aa} Also at Section de Physique, Université de Genève, Geneva, Switzerland

^{ab} Also at Departamento de Física, Universidade de Minho, Braga, Portugal

^{ac} Also at Department of Physics, The University of Texas at Austin, Austin TX, United States of America

^{ad} Also at Department of Physics and Astronomy, University of South Carolina, Columbia SC, United States of America

^{ae} Also at Institute for Particle and Nuclear Physics, Wigner Research Centre for Physics, Budapest, Hungary

^{af} Also at California Institute of Technology, Pasadena CA, United States of America

^{ag} Also at Institute of Physics, Jagiellonian University, Krakow, Poland

^{ah} Also at LAL, Université Paris-Sud and CNRS/IN2P3, Orsay, France

^{ai} Also at Nevis Laboratory, Columbia University, Irvington NY, United States of America

^{aj} Also at Department of Physics and Astronomy, University of Sheffield, Sheffield, United Kingdom

^{ak} Also at Department of Physics, Oxford University, Oxford, United Kingdom

^{al} Also at Department of Physics, The University of Michigan, Ann Arbor MI, United States of America

^{am} Also at Discipline of Physics, University of KwaZulu-Natal, Durban, South Africa

* Deceased